

Aus der
Neurochirurgischen Klinik und Poliklinik
Klinik der Universität München
Direktor: Prof. Dr. Florian Ringel

CBD as therapeutic agent for malignant glioma

Dissertation
zum Erwerb des Doktorgrades der Medizin
an der Medizinischen Fakultät
der Ludwig-Maximilians-Universität zu München

vorgelegt von
Sven Richter

aus
Gelsenkirchen

Jahr
2026

Mit Genehmigung der Medizinischen Fakultät
der Universität München

Berichterstatter: Prof. Dr. Rainer Glaß
Mitberichterstatter: PD Dr. Bogdana Suchorska
Prof. Dr. Claus Belka

Mitbetreuung durch den
promovierten Mitarbeiter: PD Dr. Roland Kälin

Dekan: Prof. Dr. med. Thomas Gudermann

Tag der mündlichen Prüfung: 12.02.2026

Table of Content

1 Table of Content

1	TABLE OF CONTENT	1
2	ABBREVIATIONS	4
3	SUMMARY	6
4	ZUSAMMENFASSUNG (DEUTSCH)	7
5	INTRODUCTION	8
5.1	GLIOBLASTOMA	8
5.1.1	CLINICAL PRESENTATION AND DIAGNOSTIC PROCEDURE	8
5.1.2	CLASSIFICATION OF GLIOBLASTOMA	9
5.1.3	COMMON AND IMPORTANT MUTATIONS IN GBM	10
5.2	CANNABIDIOL (CBD)	12
5.2.1	THERAPEUTIC APPLICATIONS OF CBD	12
5.2.2	PHARMACOLOGY OF CBD	13
5.2.3	EFFECT OF CBD ON GBM	13
5.3	NF-KB	14
5.3.1	FAMILY MEMBERS AND STRUCTURE OF NF-KB	14
5.3.2	ACTIVATION AND REGULATION OF NF-KB	15
5.4	PKCζ	17
5.4.1	PKC ζ AND ITS INTERACTION WITH NF-KB P65	17
5.5	AIM OF THIS DISSERTATION	19
6	MATERIALS	20
6.1	LABORATORY EQUIPMENT, DEVICES AND SOFTWARE	20
6.2	CONSUMABLES	21
6.3	CELL CULTURE MATERIALS	22
6.4	CHEMICALS AND REAGENTS	22
6.5	ASSAY KITS	23
6.6	ANTIBODIES	23
6.6.1	PRIMARY ANTIBODIES	23
6.6.2	SECONDARY ANTIBODIES	23
6.6.3	STREPTAVIDIN CONJUGATES	23
6.7	GBM CELL LINES	24
7	METHODS	25
7.1	CELL CULTURING	25
7.2	MEDIUM CHANGES	25
7.3	PASSAGING CELLS	25
7.4	CELL COUNTING	26
7.5	CYTOTOXICITY ASSAY	26
7.6	MTT ASSAY	27
7.7	IMMUNOCYTOCHEMISTRY	28

Table of Content

7.8	STATISTICAL EVALUATION.....	30
8	<u>RESULTS</u>	<u>31</u>
8.1	INHIBITION OF IKK WITH ACHP TO PREVENT NUCLEAR TRANSLOCATION OF NF-KB	31
8.2	INHIBITION OF THE TRANSLOCATION OF NF-KB WITH SN50	34
8.2.1	CYTOTOXICITY ASSAY	34
8.2.2	IMMUNOCYTOCHEMISTRY	38
8.3	ROLE OF PKCζ IN SELECTED GBM CELL LINES	42
8.3.1	MTT ASSAY	42
8.3.2	IMMUNOCYTOCHEMISTRY	46
9	<u>DISCUSSION</u>	<u>50</u>
9.1	INTERPRETATION OF THE RESULTS OF THE INHIBITION OF THE TRANSLOCATION OF NF-KB	50
9.2	INTERPRETATION OF THE RESULTS OF THE INVESTIGATIONS ON PKCζ.....	51
9.3	PROSPECT FOR THE FUTURE OF CBD ON GLIBLASTOMA.....	53
10	<u>BIBLIOGRAPHY</u>	<u>55</u>

Table of Content

List of Figures

Figure 1: Structural formular of Cannabidiol (CBD)	12
Figure 2: PKC ζ and its interaction with NF- κ B p65	18
Figure 3: Relative cytotoxicity of ACHP in Line 2	32
Figure 4: Relative cytotoxicity of ACHP in NCH 644	32
Figure 5: Relative cytotoxicity of CBD after pretreatment with ACHP in Line 2	33
Figure 6: Relative cytotoxicity of CBD after pretreatment with ACHP in NCH 644	33
Figure 7: Relative cytotoxicity of NF- κ B sn50 in Line 2	34
Figure 8: Relative cytotoxicity of NF- κ B sn50 in Line 11	35
Figure 9: Relative cytotoxicity of NF- κ B sn50 in NCH 644	35
Figure 10: Relative cytotoxicity of CBD after pretreatment with NF- κ B sn50 in Line 2	36
Figure 11: Relative cytotoxicity of CBD after pretreatment with NF- κ B sn50 in Line 11	37
Figure 12: Relative cytotoxicity of CBD after pretreatment with NF- κ B sn50 in NCH 644	37
Figure 13: Immunocytochemistry of NF- κ B p65 in Line	39
Figure 14: Immunocytochemistry of NF- κ B p65 in Line 11	40
Figure 15: Immunocytochemistry of NF- κ B p65 in NCH 644	41
Figure 16: Relative viability of Line 2 after PKC ζ pseudosubstrate-treatment	43
Figure 17: Relative viability of Line 11 after PKC ζ pseudosubstrate-treatment	43
Figure 18: Relative viability of NCH 644 after PKC ζ pseudosubstrate-treatment	44
Figure 19: Relative viability of GBM 20 after PKC ζ pseudosubstrate-treatment	44
Figure 20: Relative viability of p53R172H-PDGFB after PKC ζ pseudosubstrate-treatment	45
Figure 21: Relative viability of cdkn2aKo-EGFRvIII after PKC ζ pseudosubstrate-treatment	45
Figure 22: Confocal microscopy of Line 2 with fluorescent staining of PKC ζ without and with CBD treatment.....	46
Figure 23: Confocal microscopy of Line 11 with fluorescent staining of PKC ζ without and with CBD treatment.....	46
Figure 24: Confocal microscopy of NCH 644 with fluorescent staining of PKC ζ without and with CBD treatment.....	47
Figure 25: Confocal microscopy of NCH 441 with fluorescent staining of PKC ζ without and with CBD treatment.....	48
Figure 26: Confocal microscopy of NCH 421k with fluorescent staining of PKC ζ without and with CBD treatment.....	48
Figure 27: Confocal microscopy of NCH GBM 14 with fluorescent staining of PKC ζ without and with CBD treatment.....	49

Abbreviations

2 Abbreviations

Abbreviation		Definition
ANK	-	Ankyrin Repeats
ATM	-	Ataxia Teleangiectatica Mutated
Bcl-3	-	B-cell lymphoma 3-encoded protein
BCR	-	B Cell Receptor
Ca ²⁺	-	Calcium
CBD	-	Cannabidiol
CB1	-	Cannabinoid Receptor 1
CB2	-	Cannabinoid Receptor 2
CDKN2A	-	Cyclin-Dependent Kinase Inhibitor 2A
CDKN2B	-	Cyclin-Dependent Kinase Inhibitor 2B
CNS	-	Central Nervous System
CBP	-	CREB-binding Protein
DAG	-	Diacylglycerol
DAPI	-	4',6-Diamidin-2-phenylindol
DNA	-	Desoxyribonucleic Acid
ECS	-	Endogenous Cannabinoid System
EGFR	-	Epidermal Growth Factor Receptor
EMA	-	European Medicine Agency
GBM	-	Glioblastoma multiforme
GLP	-	G9A-like protein
GPCR	-	G-Protein coupled Receptor
GPR55	-	G-Protein coupled Receptor 55
Gy	-	Gray
H3K9	-	Histone H3 Lysine 9
IDH1	-	Isocitrate Dehydrogenase-1
IKK	-	Inhibitor of kappa-B Kinase
IκB	-	Inhibitor of kappa-B
IL-1R	-	Interleukin 1 Receptor
LTβR	-	Lymphotoxin B receptor

Abbreviations

MRI	-	Magnetic Resonance Imaging
MS	-	Multiple Sclerosis
nAChR α -7	-	Nicotinic Acetylcholine Receptor α 7
NF- κ B	-	Nuclear Factor kappa-B
NF1	-	Neurofibromin
NIK	-	NF- κ B Inducing Kinase
PDGF	-	Platelet-Derived Growth Factor
PDGFRA	-	Platelet-Derived Growth Factor Receptor α
PKC	-	Protein Kinase C
RANK	-	Receptor Activator of Nuclear Factor kappa-B
RelA	-	NF- κ B p65
RHD	-	Rel Homology Domain
RTK	-	Receptor Tyrosine Kinase
SETD6	-	SET Domain-containing 6
TAD	-	Transactivation Domain
TERT	-	Telomerase Reverse Transcriptase
THC	-	Delta-9 Tetrahydrocannabinol
TLR	-	Toll-Like Receptor
TMZ	-	Temozolomide
TNFR	-	Tumor Necrosis Factor Receptor
TP53	-	Tumor Protein p53
TRP	-	Transient Receptor Potential
TRPA1	-	Transient Receptor Potential Ankyrin Type 1
TRPM8	-	Transient Receptor Potential Melastin Type 8
TRPV1	-	Transient Receptor Potential Vanilloid Type 1
WHO	-	World Health Organization
2-AG	-	2-Arachidonoyl Glycerol
5-ALA	-	5-Aminolevulinic Acid
5-HT _{1A}	-	Serotonin Receptor 1A

Summary

3 Summary

Glioblastoma is a highly aggressive and malignant tumor with an inauspicious prognosis. Its rapid proliferation and invasive properties can, at least in part, be attributed to the transcription factor NF- κ B. The cannabinoid cannabidiol has been shown to exert a cytotoxic effect in certain cannabidiol-sensitive glioblastoma cells. Interestingly, while cannabidiol promotes the nuclear accumulation of NF- κ B, it simultaneously inhibits its phosphorylation at serine 311, which is an essential modification for its function as a transcription factor.

In the first part of this publication, the relevance of NF- κ B translocation was examined in more detail. Cytotoxicity assays demonstrated that co-application of the NF- κ B sn50 inhibitor completely abolished the cytotoxic effect of cannabidiol, indicating that NF- κ B translocation is essential for mediating the cytotoxic response to cannabidiol. Supporting this, immunocytochemical staining revealed that the inhibitor effectively prevented NF- κ B from translocating into the nucleus in the same cells. These findings suggest that translocation and consecutive nuclear accumulation of NF- κ B lacking phosphorylation at serine 311 is critical for the cytotoxic effect of cannabidiol in cannabidiol-sensitive glioblastoma cells.

The second part of this publication further investigated the role of protein kinase C zeta in glioblastoma cells, given its ability to phosphorylate NF- κ B at serine 311, a modification critical for transcriptional activity related to cell survival. Viability assays demonstrated that PKC ζ is present in glioblastoma cells, as evidenced by a reduction in cell numbers following the application of a PKC ζ pseudosubstrate. This observation was further confirmed by immunocytochemical staining. However, CBD application led to varying effects on PKC ζ expression across the investigated cell lines, with some showing increased expression, others unchanged levels, and some a reduction.

4 Zusammenfassung (Deutsch)

Das Glioblastom ist ein hochaggressiver und maligner Tumor mit infauster Prognose. Die aggressive und invasive Proliferation des Glioblastoms kann unter anderem auf den Transkriptionsfaktor NF- κ B zurückgeführt werden. Das Cannabinoid Cannabidiol kann bei bestimmten Cannabidiol-sensitiven Glioblastomzellen einen zytotoxischen Effekt hervorrufen. Dabei bewirkt Cannabidiol, dass in jenen Zellen NF- κ B im Nukleus verstärkt akkumuliert. Die für die Funktion von NF- κ B als Transkriptionsfaktor wichtige Phosphorylierung an Serin 311 wird jedoch unterbunden.

In dem ersten Teil wurde die Bedeutung der Translokation von NF- κ B genauer eruiert. Dabei konnte in Zytotoxizitätsassays gezeigt werden, dass durch die gleichzeitige Applikation des Inhibitors NF- κ B sn50 der zytotoxische Effekt von Cannabidiol aufgehoben werden konnte. Ergänzend konnte in immunozytochemischen Färbungen gezeigt werden, dass in den gleichen Zellen der Inhibitor die Translokation von NF- κ B in den Nucleus verhinderte. Daraus konnte die Schlussfolgerung gezogen werden, dass die Translokation von NF- κ B für den zytotoxischen Effekt von Cannabidiol in Cannabidiol-sensitiven Zellen essenziell ist, da es nur dadurch zur nukleären Akkumulation von NF- κ B ohne Phosphorylierung an Serin 311 kommt.

Im zweiten Teil wurde die Rolle von PKC ζ in Glioblastomzellen weiter eruiert. PKC ζ phosphoryliert NF- κ B an Serin 311, welche für die transkriptionelle Aktivität von NF- κ B in Hinsicht auf das Zellüberleben essenziell ist. In Viabilitätsassays konnte gezeigt werden, dass PKC ζ in den Glioblastomzellen vorhanden ist, indem nach Applikation eines PKC ζ -Pseudosubstrates eine reduzierte Zellzahl zu beobachten war. Dieser Fund konnte in immunzytochemischen Färbungen verifiziert werden. In den verschiedenen Zellreihen zeigt sich dabei jedoch kein einheitliches PKC ζ Expressionsmuster nach CBD-Applikation.

5 Introduction

5.1 Glioblastoma

Glioblastoma (GBM), formerly known as Glioblastoma multiforme, is a neuroepithelial-derived brain tumor (Rivera et al 2008). Due to its invasive and destructive growth the World Health Organization (WHO) classifies GBM as a CNS WHO grade 4 tumor (Louis et al 2021). It is the most common, malignant and aggressive primary brain tumor, accounting for 14.7% of all brain and central nervous system (CNS) tumors, for 47.7% of all primary malignant CNS tumors and 56.6% of all astrocytic tumors (Ostrom et al 2018). The annual incidence rate is 3.21 per 100,000, with men being affected slightly more frequently than women (1.58:1) (Ostrom et al 2018). GBM can occur in children as well as in adults with an average age of 65 when diagnosed (Ostrom et al 2018). Despite standard therapy consisting of neurosurgical resection followed by radiotherapy (60 Gy in 30 fractions) and either concomitant or adjuvant chemotherapy with temozolomide (TMZ), survival remains poor with an average survival of 14 months and a 5-year survival rate of 5.6% (Hanna et al 2020, Ostrom et al 2018). Last major therapeutical changes have been the introduction of postoperative radiochemotherapy in the clinical routine in 2005 and the improvement of surgery techniques like utilizing 5-aminolevulinic acid (5-ALA) to detect tumor tissue and intraoperative Magnetic Resonance Imaging (MRI) (Eljamel & Mahboob 2016, Eriksson et al 2019, Jenkinson et al 2018). But after the introduction of temozolomide more than 15 years ago, there has been no appreciable progress from a pharmacological point of view (Stupp et al 2005). Even promising approaches such as the angiogenesis inhibitor Bevacizumab failed to show a survival benefit (Gilbert et al 2014). Therefore, new and more effective pharmacological options are needed (Aldape et al 2019).

5.1.1 Clinical Presentation and Diagnostic Procedure

Patients with GBM do not show specific initial symptoms. The symptoms reported at initial consultation with a physician are either due to direct impairment of brain areas or increased intracranial pressure, which is due to the peritumoral edema (Liu et al 2013, Wen et al 2020). The most commonly reported initial symptom is headache, which can vary widely depending on the size and location of the tumor. Especially in combination with other neurological symptoms or deficits the probability for the presence of a brain tumor increases (McKinnon et al 2021). The second most common initial symptom is an epileptic seizure (McKinnon et al

Introduction

2021). Other possible complaints are nausea, dizziness, lethargy, focal neurological deficits, stroke-like symptoms, loss of memory or personality changes (Young et al 2015).

The diagnosis of GBM is confirmed by contrast-enhanced cranial MRI. Here, GBM typically presents as a necrotic area with marginal contrast agent uptake and peritumoral edema (Wen et al 2020). To further classify the tumor, a sample of the tumor tissue is needed, which can be obtained either by surgery or, if this is not an option for a patient, by biopsy (Weller et al 2017).

5.1.2 Classification of Glioblastoma

According to the WHO classification of tumors of the central nervous system (WHO CNS5) Glioblastoma, isocitrate dehydrogenase (IDH) wildtype are classified as CNS WHO grade 4, which is the highest stage within the classification (Louis et al 2021). This classification, which classifies all tumors of the brain and spinal cord, is based primarily on histopathologic appearance and molecular genetic patterns. Especially in the latest version of this classification the importance of molecular diagnostics is emphasized (Louis et al 2021). With respect to GBM, IDH-wildtype this means that diagnostic criteria include not only the classic pathologic findings, microvascular proliferation, or necrosis, but also when any of three specific molecular alterations are present. These include Telomerase Reverse Transcriptase (TERT) promoter mutation, or Epidermal Growth Factor Receptor (EGFR) gene amplification, or chromosome 7 amplification and chromosome 10 loss (+7/-10) (Louis et al 2020). Therefore, molecular testing should be performed as part of standard diagnostics for accurate diagnosis and to guide appropriate treatment decisions (Louis et al 2020, Sejda et al 2022).

Molecularly, 3 different subtypes of GBM can be distinguished (Mao et al 2022). These include the classical, the mesenchymal and the proneural subtype (Jankowska et al 2021, Verhaak et al 2010). The classic subtype shows a high rate of chromosome 7 amplification and chromosome 10 loss (+7/-10) commonly combined with alterations in the EGFR gene, but a lack of TP53 mutation. Also molecular alterations can occur in the CDKN2A, RB1, CDK4, CCDN2, NOTCH3, JAG1, LFNG, SMO, GAS1 and GLI2 gene (Jankowska et al 2021, Verhaak et al 2010). In the mesenchymal subtype alteration in the Neurofibromin (NF1) gene is common, but also alterations in the PTEN, AKT, MET, CHI3LI, TP53, TRADD, RELB and TNFRSF1A genes can occur. Additionally mesenchymal and astrocytic markers like CD44 and MERTK can be found (Jankowska et al 2021, Verhaak et al 2010). In the proneural subtype alterations in PDGFRA

Introduction

and IDH1 are dominant. Further mutations in the TP53, PIK3CA/PIK3RI, HIF, CDKN1A, NKX2-2, OLIG2, SOX, DCX, DLL3, ASCL1 and TCF4 gene are commonly present (Jankowska et al 2021, Verhaak et al 2010). Previously, the neural subtype was described containing fewer specific mutations, including alterations in the NEFL, GABRA1, SYT1, SLC12A5 and TP53 genes (Jankowska et al 2021, Verhaak et al 2010). Recent results, however, indicate that the neural subtype is more likely an artifact, representing non-tumor specific changes (Wang et al 2017).

5.1.3 Common and important mutations in GBM

The EGFR gene encodes the homonymous protein, the transmembrane EGFR, a receptor tyrosine kinase of the ERBB family. This can form homodimers after binding of one of its ligands and, through its activation, stimulate cell survival and proliferation, but also cell migration and invasion (Chakravarti et al 2004, Roskoski 2014). Mutations of the EGFR are common in GBM and are especially characteristic for the classical subtype (Brennan et al 2013, Verhaak et al 2010). The most common of its mutations in GBM is the EGFRvIII variant (Aldape et al 2004). Structural changes prevent EGFRvIII from binding ligands and instead remains constitutively active (Guo et al 2015). Although EGFR is part of a common and significant pathway, targeted therapies with EGFR tyrosine kinase inhibitors have not been effective (Le Rhun et al 2019).

The tumor suppressor gene TP53 encodes the transcription factor p53. This protein plays an important regulatory role in the cell cycle by activating the expression of genes involved in DNA repair, cell cycle regulation and induction of apoptosis when DNA damage is present (Zhang et al 2018). Alterations in the p53 pathway are present in the majority of GBM, often due to alteration of TP53 (Brennan et al 2013). Dysfunction of the p53 pathway leads to less apoptosis and more proliferation. In combination with other genetic alterations, it drives GBM progression (Zhang et al 2018).

Cyclin-dependent kinase inhibitor 2A (CDKN2A) is a gene encodes for the proteins p14^{ARF} and p16^{INK4a}. Cyclin-dependent kinase inhibitor 2B (CDKN2B) encodes for the protein p15^{INK4b}. These tumor suppressors regulate the cell cycle, consequently mutations in the genes lead to uncontrolled cell proliferation (Funakoshi et al 2021, Gil & Peters 2006). Deletion in CDKN2A

Introduction

is the most common reason for dysregulation in p53 signaling pathway in GBM (Brennan et al 2013).

Platelet-derived growth factor receptor α (PDGFRA) is a members of the receptor tyrosine kinase (RTK) family. It is encoded by the PDGFRA gene. Activation of the receptor ultimately promotes cell survival, differentiation and proliferation (Guérit et al 2021). Alterations of PDGFRA are dominant in the proneural subtype (Verhaak et al 2010) and play an important role in tumorigenesis and progression (Gai et al 2022). However, targeted therapy with antibody against PDGFRA failed to induce antitumor effect (Gai et al 2022).

The Neurofibromatosis type 1 (NF1) gene codes for the protein Neurofibromin 1, a GTPase-activating protein, which downregulates GTP-bound RAS by stimulating its intrinsic GTPase activity. Hence, the loss of function of NF1 supports uncontrolled growth and cell proliferation (Philpott et al 2017). Mutations in NF1 are predominantly present in the mesenchymal subtype (Verhaak et al 2010).

O6-methylguanine-DNA methyltransferase (MGMT) promoter status is a stratification marker with therapeutic and prognostic relevance (Hegi et al 2005). MGMT is part of the DNA repair system and removes unintended alkyl groups from O6 guanine of DNA. Methylation of the promoter results in decreased expression of MGMT and consequent accumulation of methylated DNA at O6 position of guanine (Watts et al 1997). It has been shown that silencing of the MGMT promoter by methylation is associated with a better response to the alkylating agent temozolomide and longer survival (Hegi et al 2005).

IDH catalyzes the oxidative decarboxylation of isocitrate and is best known for its role in the citrate cycle (Han et al 2020). IDH-wildtype is a defining criterion for GBM, IDH-wildtype (Louis et al 2021, Songtao et al 2012). In contrast, mutations of IDH occur in astrocytoma, IDH-mutant, which can be classified as CNS WHO grade 2,3 or 4, as well as in oligodendroglioma, IDH-mutant, which can be classified as CNS WHO grade 3 or 4 (Louis et al 2021, Songtao et al 2012). Mutated IDH causes the accumulation of the oncometabolite D-2-hydroxyglutarate. Simultaneously, impaired function of the citrate cycle occurs (Han et al 2020).

Introduction

5.2 Cannabidiol (CBD)

Cannabidiol (CBD) is one of 125 phytocannabinoids extracted from the female hemp plant, *Cannabis sativa*, and accounts for up to 40 percent of the plant's extract (Campos et al 2012, Radwan et al 2021). However, compared to the other most abundant cannabinoid delta-9 tetrahydrocannabinol (THC), CBD is a non-intoxicating agent (Hindocha et al 2015). CBD, which was first isolated in 1940, has increasingly become the focus of current research after the endogenous cannabinoid system was described in 1991 (Adams et al 1940, Burstein 2015, Devane et al 1992).

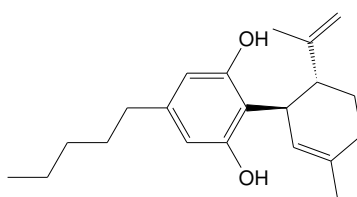


Figure 1: Structural formular of Cannabidiol (CBD) (Created with mol2chemfig 2022, after alignment with PubChem 2022)

5.2.1 Therapeutic Applications of CBD

Documentation on the medicinal use of cannabis can already be found in the oldest pharmacopoeia, the *pen-ts'ao ching*. It reports that cannabis was used in ancient China as early as 2700 B.C. to treat rheumatic pain, intestinal constipation, disorders of the female reproductive system, as well as infectious diseases such as malaria (Zuardi 2006). When cannabis for medicinal purposes was introduced to Europe in the mid-19th century, it was used to treat rheumatic diseases, epileptic seizures, as well as muscle spasms associated with rabies and tetanus (Zuardi 2006).

Until today, a wide range of therapeutic possibilities has been discovered. Among other things, CBD has been proven to have anxiolytic (Blessing et al 2015), anti-psychotic (McGuire et al 2018), anti-epileptic (Devinsky et al 2016) and spasmolytic effects (Riva et al 2019). Thus, a reduction in the frequency of seizures has been demonstrated in children with therapy-resistant seizures in Dravet syndrome or in patients of all ages with Lennox-Gastaut syndrome (Devinsky et al 2017, Devinsky et al 2018). For this, purified CBD, *Epidyolex*[®], received its approval by the European Medicines Agency (EMA) in 2019 (ema.europa.eu 2021). Another established field of application is the treatment of spasticity in patients with multiple sclerosis (MS) (Collin et al 2007). Here, Nabiximol, *Sativex*[®], which has a 1:1 ratio of CBD to THC, can be

Introduction

applied oromucosally (Vermersch & Trojano 2016). Overall, CBD has a favorable side effect profile and is well tolerated by most patients. Commonly reported adverse effects are drowsiness or fatigue (Huestis et al 2019, Iffland & Grotenhermen 2017). This, combined with CBD's versatile effects, is spurring research into finding other potential applications.

5.2.2 Pharmacology of CBD

The two main receptors of the endogenous cannabinoid system (ECS) are cannabinoid receptor 1 (CB1) and 2 (CB2), which are both G-protein coupled receptors (GPCR) (Houston & Howlett 1993, Munro et al 1993). CB1 is mainly located in the CNS, whereas CB2 can be found in the glial cells as well as peripheral localized leukocytes (Howlett 2002, Miranzadeh Mahabadi et al 2021). Two main endocannabinoids that bind to the receptors are arachidonoyl ethanolamide (anandamide) and 2-arachidonoyl glycerol (2-AG) (Devane et al 1992, Mechoulam et al 1995). Of the phytocannabinoids, THC shows a strong effect as an agonist at CB1 and CB2 (Huestis et al 2001), while CBD shows an antagonistic effect at both receptors (Thomas et al 2007). Although the exact mechanisms of action of CBD are still unclear, there have been described a variety of targets on which CBD exerts an effect. These include agonism at Transient Receptor Potential (TRP) channels like TRP Vanilloid Type 1 (TRPV1), TRP Ankyrin Type 1 (TRPA1) or TRP Melastin Type 8 (TRPM8) (Bisogno et al 2001, De Petrocellis et al 2008), Glycine Receptor α 1, α 1 β and α 3 (Ahrens et al 2009, Xiong et al 2012) and Serotonin Receptor 1A (5-HT_{1A}) (Russo et al 2005) as well as antagonism at G-protein Coupled Receptor 55 (GPR55) (Ryberg et al 2007) and Nicotinic Acetylcholine Receptor α 7 (nAChR α -7) (Mahgoub et al 2013). In addition, CBD shows a direct inhibitory effect on T-type calcium channels and voltage-dependent sodium currents (Ghovanloo et al 2018, Ross et al 2008). Furthermore, CBD interacts with many enzymes and proteins, including many of the cytochrome P450 family (Ibeas Bih et al 2015).

5.2.3 Effect of CBD on GBM

Recent works in our laboratory have shown the potentially therapeutical use of cannabidiol in GBM (Nagl 2022, Volmar et al 2021). Both in vitro and in vivo, CBD induced cell death of GBM cells, and mice implanted with GBM and subsequently treated with CBD showed prolonged survival (Volmar et al 2021). It was observed that not all GBM cell lines were sensitive to CBD. Those in which CBD showed increased cytotoxic effects were categorized as CBD-responders (Volmar et al 2021). This work also provided evidence that Nuclear Factor kappa B (NF- κ B)

Introduction

plays in a crucial roles in GBM cell lines and is substantially involved in mediating the cytotoxic effect of CBD (Volmar et al 2021).

5.3 NF- κ B

The members of the NF- κ B/Rel family are proteins functioning as dimerizing transcription factors (Siebenlist et al 1994). NF- κ B was named after its first description in 1986 as a protein complex that selectively binds to and activates the enhancer region of the immunoglobulin κ light-chain gene in B cells (Sen & Baltimore 1986a, Sen & Baltimore 1986b). Now more than 30 years later, NF- κ B is known to be expressed in almost all different types of cells and tissues and NF- κ B specific binding sites can be found at promoter and enhancer regions of more than 500 genes (Gupta et al 2010, Oeckinghaus & Ghosh 2009). Thus, NF- κ B regulates not only genes responsible for innate and adaptive immune responses but also those responsible for cell differentiation, proliferation, cell survival and stress response (Bonizzi & Karin 2004, Gerondakis et al 1999, Hayden & Ghosh 2004, Pahl 1999). Dysregulation or dysfunction of NF- κ B can lead to a variety of pathologies such as diabetes, liver disease or cancer (Dolcet et al 2005, Pasparakis et al 2006).

5.3.1 Family Members and Structure of NF- κ B

The NF- κ B/Rel family comprises a total of five members. These include RelA (p65), RelB, c-Rel, NF- κ B1 (p50) and NF- κ B2 (p52) (Oeckinghaus & Ghosh 2009). Together, these form homo- and heterodimers in particular combinations, of which p65/p50 is by far the most common (Oeckinghaus & Ghosh 2009). For dimerization, a special region, the Rel Homology Domain (RHD), which is localized towards the amino-terminus and is about 300 amino acids long, is present in all five proteins. In addition, the RHD is critical for interaction with inhibitor of nuclear factor kappa B ($\text{I}\kappa\text{B}$) proteins, translocation to the nucleus, and eventually binding to DNA (Oeckinghaus & Ghosh 2009). RelA, RelB and c-Rel also possess a transactivation domain (TAD), which is localized towards the carboxy-terminus and is necessary to recruit coactivators and displace repressors (Hayden & Ghosh 2004). Therefore, an NF- κ B dimer must obtain at least one of these three proteins to initiate transcription at the DNA (Hayden & Ghosh 2012). RelB uniquely possesses a leucine zipper region at the amino-terminus in addition to the TAD, which is required for full active function (Dobrzanski et al 1993). P50 and p52, on the other site, lack in TAD. Instead, they contain several carboxy-terminal located ankyrin repeats (ANK),

Introduction

which inhibit nuclear translocation and DNA binding, providing them the function of I κ B proteins (Mussbacher et al 2019, Naumann et al 1993, Rice et al 1992). Homo- and heterodimers consisting of p50 and p52 therefore act as repressors for κ B-dependent transcription (Zhong et al 2002). P50 is processed from its precursor p105 by the 20S proteasome (Moorthy et al 2006), whereas p52 is processed by proteolytic cleavage from its precursor p100 (Heusch et al 1999). The precursors p105 and p100 are also classified as I κ B proteins (Oeckinghaus & Ghosh 2009).

Post-translational protein modifications of NF- κ B subunits are important for optimal NF- κ B response. These include acetylation, ubiquitination and especially phosphorylation (Hochrainer et al 2013, Oeckinghaus & Ghosh 2009). Since NF- κ B p65 possesses the strongest transcriptional potential (Schmitz & Baeuerle 1991), its post-translational phosphorylations have been well mapped. These phosphorylation sites (phospho-sites), containing serine (ser) or threonine (thr), can be found all over the molecule. Four phospho-sites (ser-205, thr-254, ser-276 and ser-281) are contained within the amino-terminal RHD (Anrather et al 1999, Ryo et al 2003), two more (ser-311 and ser-316) are located carboxy-terminally to the RHD (Duran 2003, Wang et al 2015) and further six (thr-435, ser-468, thr-505, ser-529, ser-536 and ser-547) are found in the carboxy-terminal TAD (O'Shea & Perkins 2010, Perkins 2006, Sabatel et al 2012). Phosphorylation of these phospho-sites results in modulation of transcriptional activity (Christian et al 2016).

5.3.2 Activation and Regulation of NF- κ B

In cells in which the NF- κ B signaling pathway is predominantly inactive, NF- κ B proteins are chaperoned by kappa B (I κ B) proteins and sequestered in the cytoplasm (Oeckinghaus & Ghosh 2009). Overall, there are eight different I κ B family members: the typical I κ B α , I κ B β and I κ B ϵ , the precursor p100 and p105, as well as the atypical members B-cell lymphoma 3 (BCL-3), I κ B ζ , and I κ BNS (Hayden & Ghosh 2012). They all share five to seven ANK toward the carboxy-terminus, which can interact with the RHD of NF- κ B proteins (Oeckinghaus & Ghosh 2009). While the typical I κ Bs fulfill their classical inhibitory function mainly in the cytosol, atypical I κ Bs interact with DNA-bound NF- κ B to modify transcription activity (Hayden & Ghosh 2012).

Introduction

NF- κ B can be activated via two pathways: the canonical and non-canonical pathways. In the canonical pathway the most abundant NF- κ B heterodimer, consisting of NF- κ B p65 and p50, is bound by a typical I κ B, mostly I κ B α (Huxford et al 1998, Jacobs & Harrison 1998). I κ B α sequesters the two subunits, masking the nuclear localization signal (NLS) of p65 but not the NLS of p50 (Huxford et al 1998). I κ B α possesses a nuclear export sequence (NES), thereby enabling continuous shuttling of the I κ B α /NF- κ B complex between the cytosol and the nucleus. However, the majority of the I κ B α /NF- κ B complex is located within the cytoplasm (Arenzana-Seisdedos et al 1997, Huxford et al 1998). The I κ B β /NF- κ B complex, on the other side, does remain in the cytosol without shuttling as long as the complex remains inactivated (Malek et al 2001).

Multiple intracellular and extracellular stimuli can lead to initiation of the canonical pathway. Possible activation pathways include Tumor Necrosis Factor Receptor (TNFR1), T Cell Receptor (TCR), B Cell Receptor (BCR), Interleukin 1 Receptor (IL-1R) or Toll-Like Receptor (TLR), but also Ataxia Teleangiectatica Mutated (ATM), which is induced by DNA damage (Yu et al 2020). After activation by their respective ligands and propagation of the signal through the respective downstream receptor-internal signaling pathway, all result in activation of the inhibitor of kappa kinase (IKK) complex (Yu et al 2020). The IKK complex consists of three subunits, the two kinases IKK α and IKK β and the regulatory subunit NF- κ B Essential Modulator (NEMO, IKK γ) (Yamaoka et al 1998). Within the complex NEMO is crucial for the activation of IKK β (May et al 2000), which in turn is important for the phosphorylation of I κ B proteins (Huber et al 2002). The phosphorylation leads to ubiquitinylation and consecutive proteasomal degradation of I κ B (Li et al 1995), which eventually releases NF- κ B, enabling unrestricted translocation into the nucleus and DNA binding (Huber et al 2002).

In the non-canonical pathway, the NF- κ B heterodimer RelB/p52 plays a crucial role (Sun 2011). RelB is initially bound to the precursor p100, which inhibits nuclear translocation and DNA binding activity (Naumann et al 1993).

The non-canonical signaling pathway can be initiated by different receptors, which all belong to the TNFR superfamily. These include the B-cell activating factor receptor (BAFFR), CD40, lymphotoxin β -receptor (LT β R), receptor activator for nuclear factor κ B (RANK) and Fn14 (Sun 2011). Activation of any of these receptors leads to recruitment of TNF receptor-associated factor (TRAF) proteins and results in activation of NF- κ B inducing kinase (NIK) by preventing proteasomal degradation of NIK, which is constant under basal conditions (Liao et al 2004, Sun

Introduction

2011). NIK phosphorylates and thus activates IKK α (Ling et al 1998). IKK α in turn phosphorylates p100, which is subsequently ubiquitinated and proteasomally processed (Senftleben et al 2001, Xiao et al 2004). The no longer inhibited heterodimer RelB/p52 can be translocated into the nucleus and become transcriptionally active there (Sun 2011).

Last, NF- κ B is subject to post-translational modifications, in particular phosphorylations, which in the case of p65 cause an predominantly transactivation affecting effect (Christian et al 2016). Among the proteins that cause phosphorylation are, for instance, IKK β , which phosphorylates NF- κ B p65 at ser-536 (Sakurai et al 1999), Protein Kinase A (PKA), which phosphorylates NF- κ B p65 at ser-276 (Zhong et al 1997), or Protein Kinase C ζ (PKC ζ), which causes phosphorylation at ser-311 (Duran 2003).

5.4 PKC ζ

Protein Kinase C (PKC) is a family of phospholipid-dependent serine/threonine kinases involved in signal transduction downstream of receptors (Kang et al 2012). In total, at least 11 different isoforms are known. The isoforms of PKC can be divided into three groups: the conventional PKCs, which are Diacylglycerol (DAG) Ca²⁺-dependent, the novel PKCs, which are Ca²⁺-independent, but still require DAG and the atypical PKCs, which require neither DAG nor Ca²⁺. PKC ζ is considered as one of the atypical PKCs (Donson et al 2000, Kang et al 2012).

It has been shown that elevated protein level of PKC ζ occur in human GBM cell lines (Xiao et al 1994). In non-proliferating cells, PKC ζ is primarily localized in the cytoplasm. In proliferating cells, active PKC ζ translocates to the nucleus (Kiley & Parker 1995, Umar 2000). Furthermore, PKC ζ is crucial for proliferation and cell growth in GBM (Donson et al 2000).

5.4.1 PKC ζ and its interaction with NF- κ B p65

PKC ζ influences the NF- κ B pathway at several sites. On the one hand, activated PKC ζ can activate IKK (Lallena et al 1999, Savkovic et al 2003), on the other hand, PKC ζ is crucial for phosphorylation of NF- κ B p65 at ser-311 (Duran 2003).

In unstimulated cells, NF- κ B p65 is a substrate of SETD6 (SET domain containing 6), a protein lysine methyltransferase (PKMT) that monomethylates NF- κ B p65 at lysine 310 (lys-310). The ANK domain of G9A-like protein (GLP) can specifically recognize and bind this methylated lys-310 (Levy et al 2011). GLP, in turn, forms heterodimers together with G9a, which methylates

Introduction

euchromatin at histones H3 Lys 9 (H3K9), thereby repressing transcriptional activity of NF- κ B p65 (Levy et al 2011, Tachibana et al 2005).

In the context of activating the NF- κ B pathway, PKC ζ , which is able to phosphorylate NF- κ B p65 at ser-311, can also be activated and is translocated into the Nucleus (Duran 2003, Umar 2000, Yao et al 2010). Phosphorylation of ser-311 prevents the ability of GLP to bind to lys-310 (Levy et al 2011). Furthermore, phosphorylated ser-311 promotes CREB-binding Protein (CBP) binding, a transcriptional coactivator with histone acetyltransferase activity, which acetylates lys-310 as well as histones. These acetylations promote transcription due to the relaxed chromatin structure (Duran 2003, Rimessi et al 2013, Yao et al 2010).

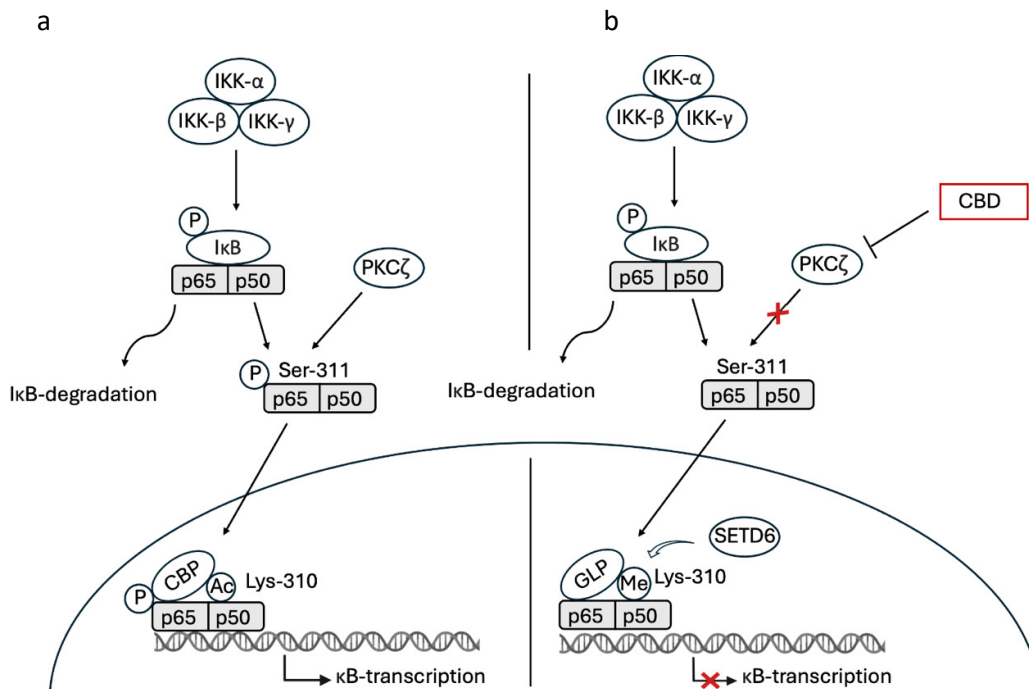


Figure 2: PKC ζ and its interaction with NF- κ B. (a) Upon activation, the IKK complex phosphorylates I κ B, which is subsequently ubiquitinated and then degraded by the proteasome. Then, NF- κ B p65 is phosphorylated by PKC ζ at serine 311 (Ser-311) and translocates into the nucleus. Phosphorylation at Ser-311 inhibits GLP binding to Lys-310 and promotes the binding of CBP, a transcriptional coactivator with histone acetyltransferase activity. CBP acetylates Lys-310 and histones, leading to a relaxed chromatin structure and enhanced transcription. (b) Under basal conditions (and without phosphorylation by PKC ζ , respectively), NF- κ B p65 is monomethylated at lysine 310 (Lys-310) by SETD6, a protein lysine methyltransferase. The ANK domain of GLP specifically recognizes and binds this methylated Lys-310. GLP forms heterodimers with G9a, which methylates histone H3 at Lys 9 (H3K9), thereby repressing NF- κ B p65 transcriptional activity. (created with Microsoft® PowerPoint, single elements extracted from © 2024 BioRender).

Introduction

5.5 Aim of this Dissertation

GBM is an aggressive malignancy with a poor prognosis, in which NF- κ B has been shown to play a crucial role. CBD, which has been established in recent years as a therapeutic agent for neurological diseases and at the same time has a favorable risk profile, has been shown to have a cytotoxic effect on GBM cells. CBD was shown to cause translocation of NF- κ B into the nucleus.

The first part of this work addresses the question of whether translocation of NF- κ B into the nucleus is crucial for the cytotoxic effect of CBD in CBD-sensitive GBM cell lines. For this purpose, cytotoxicity assays were performed and tested by immunocytochemistry.

In the second part, we investigated whether PKC ζ , the protein kinase that can phosphorylate NF- κ B at ser-311, is present in GBM cell line. For this purpose, viability assays were performed and verified by immunocytochemistry.

Materials

6 Materials

6.1 Laboratory Equipment, Devices and Software

Equipment / Device / Software	Company	Type / Cat. Number
Axiovision rel. 4.8 / 4.9 software	Zeiss	
Centrifuge	Thermo Scientific	Heraeus Multifuge 1S
Digital orbital shaker	Biozym	HSB02159
Dry incubator	Thermo Scientific	Heraeus B6
Fluorescence microscope	Zeiss	
GraphPad Prism	GraphPad Software, Inc.	
HERA safe hood	Thermo Scientific	KS 12
Humid incubator	Binder	9040-0038
ImageJ	Wayne Rasband	
Inverted trinocular microscope	hund	Wilovert S
Las X software	Leica Microsystems	
Leica inverted confocal microscope	Leica Microsystems	DMI8
Micropipette (10, 20, 200 and 1000 µl)	Eppendorf	Eppendorf Research plus (3123000020, 3123000098, 3123000055, 3123000063)
Microsoft Office	Microsoft	Excel
Multimode microplate Reader	Tecan	Infinity® 200 PRO
Pipettor	Integra	Pipetboy comfort
Refrigerators (4°C, -20°C)	Liebherr	
Stepper	Eppendorf	Multipipette® Plus
Vortex mixer	VWR	12-620-856
Water bath	Julabo	TW20

Materials

6.2 Consumables

Product	Supplier	Cat. Number
Culture slides	Falcon	354108
Cell culture flask T25	TPP	90026
Cell culture flask T75	TPP	90076
Cell culture flask T150	TPP	909151
Cell culture dish	Sigma-Aldrich	755923
Cell Strainer 70 µm	BD	352350
Combitips advanced® 1 ml	Eppendorf	0030089430
Combitips advanced® 5 ml	Eppendorf	0030089456
Cover slips	Thermo Fisher Scientific	BBAD02400500#A1
Stripette® 5 ml	Costar	CLS4487
Stripette® 10 ml	Costar	CLS4488
Stripette® 25 ml	Costar	CLS4489
Centrifuge tubes 0.5 ml	Eppendorf	0030121.023
Centrifuge tubes 1.5 ml	Eppendorf	0030121.694
Centrifuge tubes 2 ml	Eppendorf 0030121.094	0030121.094
Centrifuge tubes 15 ml	TPP / Falcon	91015
Centrifuge tubes 50 ml	TPP / Falcon	91051
Pipette tips 0.5 - 10 µl	Eppendorf	3123000020
Pipette tips 10 - 100 µl	Eppendorf	3123000047
Pipette tips 20 - 200 µl	Eppendorf	3123000055
Pipette tips 100 - 1000 µl	Eppendorf	3123000063
96-well plate	TPP	92096
384-well plate, black, flat bottom	Corning	3573

Materials

6.3 Cell Culture Materials

Material	Supplier	Cat. Number
B-27™ Supplement	Gibco	17504044
DMEM/F-12, without phenol red	Gibco	21041025
DMEM/F-12, with phenol red	Gibco	11320074
Epidermal Growth Factor (EGF)	PeptoTech	AF-100-15
Fibroblast Growth Factor (FGF)	PeptoTech	AF-100-18B
NeuroCult™ Basal Medium (Mouse)(NSC)	Stemcell Technologies	05700
NeuroCult™ Proliferation Supplement (Mouse)	Stemcell Technologies	05701
Penicillin-Streptomycin (P/S)	Gibco	15140122

6.4 Chemicals and Reagents

Chemical/Reagent	Supplier	Cat. Number
Accutase®	Gibco	A11105-01
Acetic acid	Roth	6755.2
ACHP	Tocris	4547
Cannabidiol (CBD)	GW Pharmaceuticals	
DAPI	Fluka	32670
Dimethyl sulfoxide (DMSO)	Sigma-Aldrich	D8418
Donkey Serum	Jackson ImmunoResearch	017-000-121
Fluorescence mounting medium	Dako	S3023
Laminin	Sigma-Aldrich	L2020-IMG
NF-κB sn50	Enzolifesciences	BML-P600-0005
Paraformaldehyd (PFA)	Sigma-Aldrich	30525-89-4
Phosphate-buffered saline (PBS)	Apotheke Klinikum LMU	APO-ST016
PKCζ Pseudosubstrate	Tocris	1791
Poly-D-Lysine-hydrobromid	Sigma-Aldrich	P7280

Materials

Poly-L-Ornithine-hydrobromid	Sigma-Aldrich	P3655
Sodium dodecyl sulfat (SDS)	Sigma-Aldrich	L5750
TNF α	PeptoTech	300-01A
Triton X-100	Roche Diagnostics	93418
Trypan blue	Sigma-Aldrich	T8154

6.5 Assay Kits

Kit	Supplier	Cat. Number
CytoToxFluor™	Promega	G9262
MTT Cell Proliferation Kit	Sigma-Aldrich	2128

6.6 Antibodies

6.6.1 Primary Antibodies

Antigen	Host Species	Dilution	Supplier	Cat. Number
NF- κ B p65 total	Rabbit IgG	1:400	BioLegend	622601
PKC ζ	Mouse IgG	1:125	Merck	MABC946

6.6.2 Secondary Antibodies

Conjugate	Antigen	Host Species	Dilution	Supplier	Cat. Number
Alexa Fluor® 488	Rabbit IgG	Donkey	1:400	Jackson ImmunoResearch	711-545-152
Biotinylated	Mouse	Donkey	1:250	Jackson ImmunoResearch	715-065-151

6.6.3 Streptavidin Conjugates

Conjugation	Dilution	Supplier	Cat. Number
Alexa Fluor® 488 - Streptavidin	1:500	Jackson ImmuniResearch	016-540-084

Materials

6.7 GBM Cell Lines

GBM cell lines were either obtained from patients or from genetically alternated mice. After harvesting and separating tumor cells from non-tumor cells, cells were stored in NPC medium with 5% DMSO in a liquid nitrogen freezing tank at -180°C.

GBM Cell Line	Origin	Subtype
GBM 14	human	neural
GBM 20	human	mesenchymal
Line 2	human	classical
Line 11	human	mesenchymal
NCH 421k	human	proneural
NCH 441	human	neural
NCH 644	human	proneural
Cdkn2aKO-EGFRvIII	murine	classical
P53R172H-PDGFB	murine	proneural

Methods

7 Methods

7.1 Cell Culturing

Cells were cultured in suspension with Gibco cell culture medium. If not otherwise mentioned this accords to DMEM/F-12 with phenol red with 1% P/S, 2% cell supplement B27, 10ng/ml FGF and 10 ng/ml EGF, abbreviated referred to as DMEM/F-12. Line 2 and Line 11 constituted an exception by being cultured in NSC with phenol red with 1% P/S, 10ng/ml FGF and 10ng/ml EGF and 50ml of its own medium specific proliferation supplement. Phenol red in both media indicated an acidic pH by turning from red to orange to yellow resulting from an increase of acidic metabolic and consequently indicated a decrease of nutrition within the medium. Cells in suspension were kept in cell culture flasks and incubated in a humid cell incubator at 37°C and 5% CO₂. After thawing, cells were kept in small 25 ml flasks (T25) with 5 ml medium, ordinary cell culturing in 75 ml flasks (T75) with 10 ml medium and if cells were demanded in high numbers, 150 ml flasks (T150) with 15 ml medium were utilized.

7.2 Medium Changes

A decrease of nutrition within the medium required a medium change to avoid stress-induced transcriptional changes of the molecular pattern. Changing the medium of cells was performed by transferring the entire cell suspension from the cell culture flask into a 15 ml Falcon tube. Cells adhered to the bottom of the flask were obtained by gently rinsing the bottom with PBS. The tube was centrifuged at 1400 rpm for 5 minutes. The supernatant was tipped and new medium was carefully applied to bring the cells back into suspension. The cell suspension was transferred back into the cell culture flask. If initially to many cells adhered to bottom of the flask and where no able to be obtained by rinsing, the empty flask was changed to a new one.

7.3 Passaging Cells

If cell were forming bigger cell spheres, cells needed to be split. This was accomplished by centrifuging the cells equal to the initial procedure for the medium change and tipping away the supernatant. 1 ml Accutase®, a cell dissociation reagent, was added to the cell pellet, gently mixed and incubated for 3 to 5 minutes in a water bath at 37°C. The tube was filled up with 10 ml PBS to dilute the Accutase® and was centrifuged again at 1530 rpm for 5 minutes.

Methods

The supernatant was tipped away and the respective medium was applied. Cell suspension was transferred back into the cell culture flask.

7.4 Cell Counting

To obtain a required number of cells for an assay cells needed to be counted. In order to count cells, they needed to be treated with Accutase® as described in the previous section. After centrifuging the second time and tipping away the supernatant exactly 1 ml of medium was applied to the cells. If cells were counted for one of the following experiments it is recommended to do this initially with DMEM/F-12 without phenol red. 20 µl of the cell suspension was diluted in trypan blue in a ratio of 1:1. If requested 20 µl of that solution could be further diluted in trypan blue until the demanded dilution was achieved. Diluted cell suspension was applied to a counting grid and was counted under the microscope. Only viable cells were counted. If too many cells still adhere together and appropriate counting was not possible, cell suspension was filtered by pipetting cells onto a 70 µm cell strainer. Dilution and counting were repeated with the filtered cell suspension.

7.5 Cytotoxicity Assay

In-vitro cell cytotoxicity was measured utilizing the CytoToxFluor™ cytotoxicity assay from Promega. Therefore 3,000 cells in 50 µl DMEM/F-12 without phenol red per well were seeded into a 96 well plate with flat bottom. The setup of the cytotoxicity assay required wells with the following conditions: cells with the substance/drug to be examined, cells with the vehicle control, cells initially untreated for the positive control and cell free wells filled with 100 µl of DMEM/F-12 without phenol red which were considered as a no-cell control. Each condition had involved a group of 5 replicates. All the relevant wells were framed with a layer of wells filled with 100 µl PBS to prevent desiccation. Then or later depending on the setup of the assay 50 µl of the substance/drug to be examined diluted in DMEM/F-12 without phenol red was concentration adjusted added into the wells. The covered plate was incubated in a humid cell incubator at 37°C. For the positive control 50 µl of Digitonin dissolved in deionized water with the concentration of 300 µg/ml were added to the respective wells causing a total cell lysis. For an optimal positive control, the Digitonin was added 1 hour prior to the transfer. The measuring of the cytotoxicity started with the transfer. Up to four transfers at different points

Methods

of time could be performed from a single 96 well plate enabling multiple measurements for one assay.

For the transfer, 20 µl of each well were equally pipetted into a corresponding well of a 384 well plate. Additionally, 20 µl of the CytoToxFluor™ reagent, containing the fluorogenic peptide substrate bis-AAF-R110 (bis-alanyl-alanyl-phenylalanyl-rhodamine 110) diluted in a ratio of 1:1,000 in the cytotoxicity assay buffer, was applied to those well. Gently tapping the lid of the 384 well plate encouraged a homogenous mixture for optimal outcome. The covered 384 well plate was incubated in a dry incubator at 37°C for 3 hours. After incubation the fluorescence intensity was obtained by the plate reader infinite® F200 from TECAN® with the software Magellan 7.1 SP1. The reader was set up to a wavelength of 485 nm Excitation and 520 nm Emission. Values of blank wells were subtracted from the rest.

Bis-AAF-R110 is converted in Rhodamine 110 by proteases released by dead cell. Due to the fact, that the bis-AAF-R100 substrate cannot cross the intact cell membrane of living cells and consequently cannot be converted by their protease, the fluorescent intensity is proportional to activity of the released proteases and therefore can be used to visualize the amount of cell death (Niles et al 2007).

7.6 MTT Assay

In-vitro cell viability was measured utilizing the MTT cell growth assay kit. This Assay was utilized in particular experimental setups, in which the cytotoxicity assay was not able to be determined cytotoxicity correctly for unknown reasons. Therefore, cells were plated equally to the setup of the cytotoxicity assay with 3,000 cells per 50 µl DMEM/F-12 without phenol red per well. Also, the setup of the MTT assay required the same conditions, in this case, however, each condition involved a group of 3 biological replicates. Since the cytotoxic effects of substances/drugs is demonstrated in this assay by a decreased viability, the condition with Digitonin was required to reflect a minimum of cell viability after total cell lysis. Wells were framed with a layer of wells filled with 100 µl PBS to prevent desiccation. The substance/drug diluted in DMEM/F-12 without phenol red was concentration adjusted added into the wells. The covered plate was incubated in a humid cell incubator at 37°C. 50 µl Digitonin (300 µg/1 ml deionized water) was added 1 hour prior to the begin of the measurement into the respective wells. Measuring started by pipetting 20 µl of the MTT (3-[4,5-dimethylthiazol-2-yl]-2,5-diphenyltetrazolium bromide) into each well. After gently mixing the liquid by tapping onto

Methods

the lid the covered plate was incubated in a humid cell incubator at 37°C for 3 hours. 100 µl of the solubilize solution (99.4 ml DMSO, 0.6 ml 100% acetic acid, 10 g SDS; SDS tended to precipitate so it needed to be shaken thoroughly prior to application). The plate was incubated at room temperature for 5 minutes. Black crystals appear on the bottom of the plate. Absorbance was detected using an ELISA plate reader with the wavelength 570 nm and a reference wavelength of 630 nm. Values of blank wells were subtracted from the rest.

The yellow MTT is converted to formazan by NAD(P)H-dependent oxidoreductases localized at the mitochondria of viable cell. The insoluble formazan forms crystals inside the viable cells which appear black after solubilization (Huet et al 1992). Hence, the obtained absorbance of the black crystals is proportional to the number of viable cells inside a well assuming that oxidoreductases within on cell line converting with an average consistent rate.

7.7 Immunocytochemistry

8-well cell culture chamber slides were utilized for growing cell onto an object slide. To provide an optimal adherence slides required a coating prior to seeding the cells using Poly-L-Ornithine (PLO) for Line 2 and Line 11 or Poly-D-Lysin (PDL) for NCH 644, NCH 441, NCH 421k and GBM 14 and Laminin. 100 µl of PLO or PDL in a concentration of 50 µg/ml were applied in each well and incubated in a humid cell incubator at 37°C for 24 hours. Liquid was extracted and gently washed with PBS for 5 minutes once. Laminin was applied and slides were incubated again in a humid cell incubator at 37°C for 2 hours. Laminin was extracted and 10,000 - 30,000 cells in 150 µl DMEM/F-12 without phenol red per well were seeded. In order to adhere to the coated surface of the slide, cells were incubated at 37°C for 24 - 48 hours. 2 wells were treated with 50 µl of the vehicle control, whereof one was required for the negative control of the staining. Other wells were treated with 50 µl of the substance/drug to be examined. Slides were incubated at 37°C. Possibly a second substance/drug was added later considering the adequate final concentration and adjusting the volume of the first treatment to not exceed a final volume of 200 µl in each well.

Some cell lines (NCH 441, NCH 421k and GBM 14) did not attach very well to the coated surface. To enable a better fixation the slide was centrifuged at 800 rpm for 5 minutes forcing more cells to stick to the surface when fluid was removed.

Fixations of the cells onto the slides was performed by removing the supernatant and washing the wells with PBS for 5 minutes once. To avoid detaching cells from the surface in this and all

Methods

further pipetting procedures the fluid was gently pipetted against the inner side wall of the wells. PBS was removed and 100 - 200 μ l 4% PFA was applied and incubated at room temperature for 10 minutes. Achieving an optimized fixation only freshly prepared PFA was utilized. PFA was removed and wells were washed with PBS 3 times for 5 minutes. After washing PBS was removed, the slide was air dried under the cell hood for 5-10 minutes.

Wells were washed with PBS for 5 minutes once again and after removing the PBS the protein blocking solution (0.3% TritonX-100 in PBS with 5% donkey serum) was applied and incubated at room temperature for 30 minutes. For the blocking as well as for all further incubation procedures an orbital shaker on a low-speed level was utilized for an evenly distribution of the liquid inside the wells.

The primary antibody was diluted in blocking solution and 100 μ l were applied to each well except one in which 100 μ l of blocking solution without primary antibody was applied. This well was later used as a negative control for the secondary antibody. The slide was put into a refrigerator at 4°C overnight, at least for 8 hours.

Primary antibody solution was removed and wells were washed with PBS for 5 minutes 3 times. The secondary antibody was diluted in blocking solution and 100 μ l was applied to each well. The slide was incubated for 2 hours at room temperature. An Alexa Fluor® fluorescent dye was linked to the secondary antibody.

In the stainings for PKC ζ an increase of the sensitivity was required to obtain an adequate signal under the microscope. In this case the secondary antibody was not linked to the fluorescent dye, but to biotin. The Alexa Fluor® fluorescent dye was coupled to streptavidin, a protein with 4 highly biotin-affine binding sides. After washing with PBS for 5 minutes 3 times, this conjugate was diluted in blocking solution and applied to each well. The slide was incubated at room temperature for 1 hour.

In order to visualize the nuclei in the cells DAPI was employed. Therefore, DAPI was diluted in PBS in a ratio 1:10,000. After washing with PBS for 5 minutes 3 times, 100 μ l DAPI-solution was applied to each well for 2 minutes. DAPI was removed and wells were washed again with PBS for 5 minutes 3 times.

Mounting the slides required to remove the PBS first and detaching the glass gasket second. 3-4 drops of the fluorescent mounting medium were gently applied onto the slide and a cover glass was mounted. Bubbles were not supposed to be under the cover glass. The edges of the

Methods

cover slides were sealed with transparent nail polish to prevent desiccation and to store the slide over a longer period.

Stained cells were evaluated under either a fluorescent microscope or a confocal microscope. The negative control was utilized to obtain the background intensity which was subtracted from the intensity of the other wells to eliminate the visualization of unintended background. Eventually microscopy images were analyzed with ImageJ. This software enables channel splitting and hence was utilized to evaluate protein distribution in contrast to the nuclear staining.

7.8 Statistical evaluation

All data was collected and immediately transferred into Excel sheets, where mean value and standard deviation as well as normalizations to the control group were determined. The mean value of the control group was arbitrarily set to 1 for all experiments to obtain relative results. All further statistical evaluations were performed with GraphPad PRISM 5 or 9. In each Experiment outlier were detected utilizing the Grubbs-Test. The Significance between groups was analyzed using an analysis of variance (ANOVA) with post hoc Dunnett's test. Results were considered as significant if P (P-value) <0.05. Following abbreviations are used: *: p<0.05, **: p<0.005, ***: p<0.001, ns = not significant. All graphs show mean values with standard deviation.

Results

8 Results

8.1 Inhibition of IKK with ACHP to prevent Nuclear Translocation of NF- κ B

The first part of this work focuses on the question whether NF- κ B is crucial for the cytotoxic effect of cannabidiol or not. For this purpose, different substances were tested, which were previously shown (by others) to modulate the NF- κ B signaling pathway. For the investigation of the following substances the cytotoxicity assay was used because the cytotoxic effect of cannabidiol is well represented in this assay.

To accomplish this, the first attempt to prevent translocation of NF- κ B into the nucleus was utilizing ACHP (2-amino-6-[2-(cyclopropylmethoxy)-6-hydroxyphenyl]-4-(4-piperidinyl)-3-pyridinecarbonitrile), a selective inhibitor of IKK α and IKK β . This inhibitor prevents the phosphorylation of I κ B α , which in turn prevents NF- κ B p65 from translocating to the nucleus. To this end, it was first investigated whether ACHP, at a dose that has been targeted in other work (Mia & Bank 2015), causes a cytotoxic effect on GBM cells on its own, or not. For this purpose, the cytotoxicity assay and the two cell lines Line 2 and NCH 644 were utilized. The cytotoxic effect was compared to the vehicle control with DMSO 0.01%. The cytotoxicity assays performed displayed no cytotoxic effect of ACHP in either cell lines (Figure 3 and 4).

Subsequently, in a new run 10 μ M CBD was added to the same cell lines after pretreatment with ACHP in different doses for 6 h and the cytotoxicity was measured. In CBD sensitive cell lines, including Line 2 and NCH 644, 10 μ M CBD results in a maximal cytotoxic effect. Hence, the ACHP + CBD groups were compared to the CBD group. Here, in both cell lines, Line 2 and NCH 644, pretreatment with ACHP did not prevent or decrease the cytotoxic effect of CBD (Figure 5 and 6).

Results

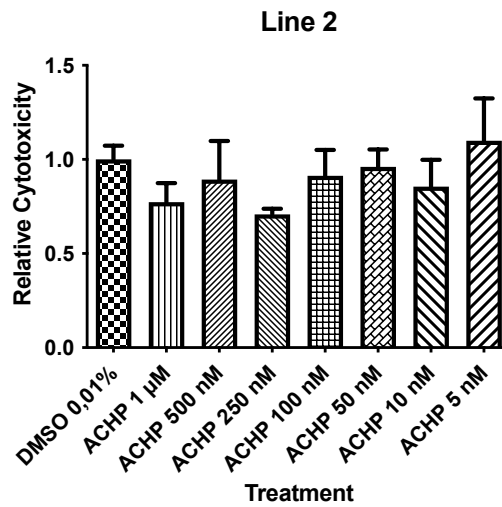


Figure 3: Relative cytotoxicity of ACHP in Line 2. 3,000 cells of Line 2 were seeded in each well. Each group consists of 5 biological replicates. ACHP was applied in 1 µM, 500 nM, 250 nM, 100 nM, 50 nM, 10 nM and 5 nM doses, vehicle control with DMSO 0.01%. Cytotoxicity was determined by TECAN® reader after 24 h. The graph demonstrates that ACHP had no significant increased cytotoxic effect in comparison with the control group on Line 2.

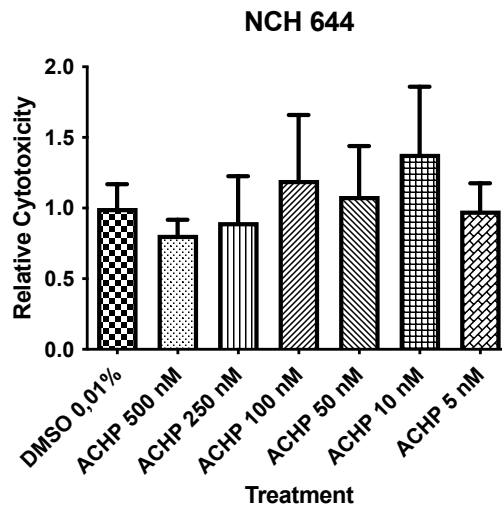


Figure 4: Relative cytotoxicity of ACHP in NCH 644. 3,000 cells of NCH 644 were seeded in each well. Each group consists of 5 biological replicates. ACHP was applied in 500 nM, 250 nM, 100 nM, 50 nM, 10 nM and 5 nM doses, vehicle control with DMSO 0.01%. Cytotoxicity was determined by TECAN® reader after 24 h. The graph demonstrates that ACHP had no significant increased cytotoxic effect in comparison with the control group on NCH 644.

Results

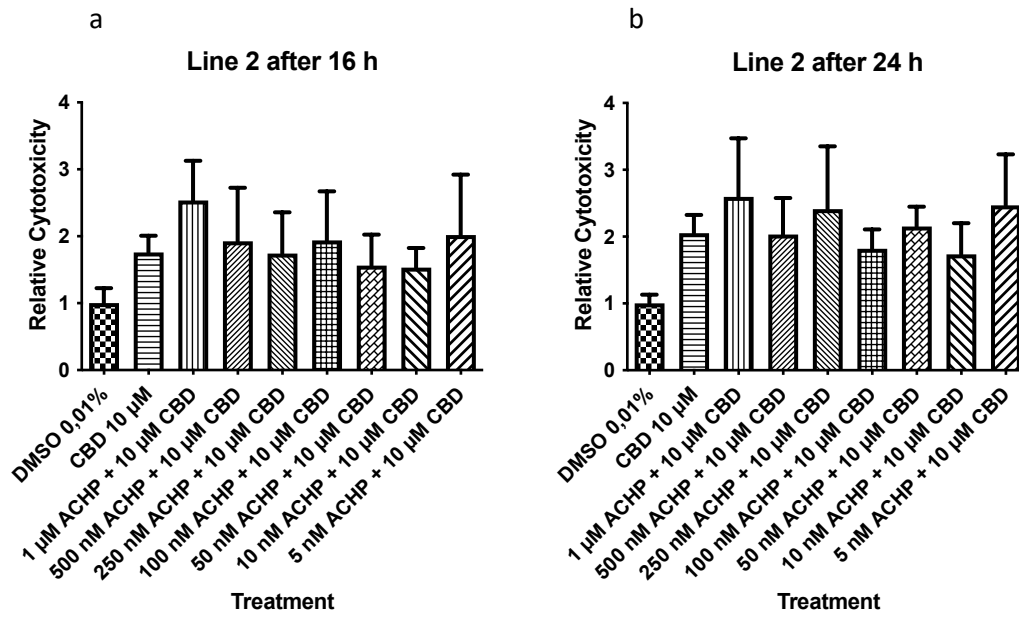


Figure 5: Relative cytotoxicity of CBD after pretreatment with ACHP in Line 2. 3,000 cells of Line 2 were seeded in each well. Each group consists of 5 biological replicates. 10 µM CBD were applied after pretreatment of 1 µM, 500 nM, 250 nM, 100 nM, 50 nM, 10 nM and 5 nM ACHP for 6 h, vehicle control was performed with DMSO 0.01%. Cytotoxicity was determined by TECAN® reader after (a) 16 h and (b) 24 h. The graphs demonstrate that neither at 16 h nor at 24 h pretreatment with ACHP prevents or decreases the cytotoxic effect of CBD on Line 2.

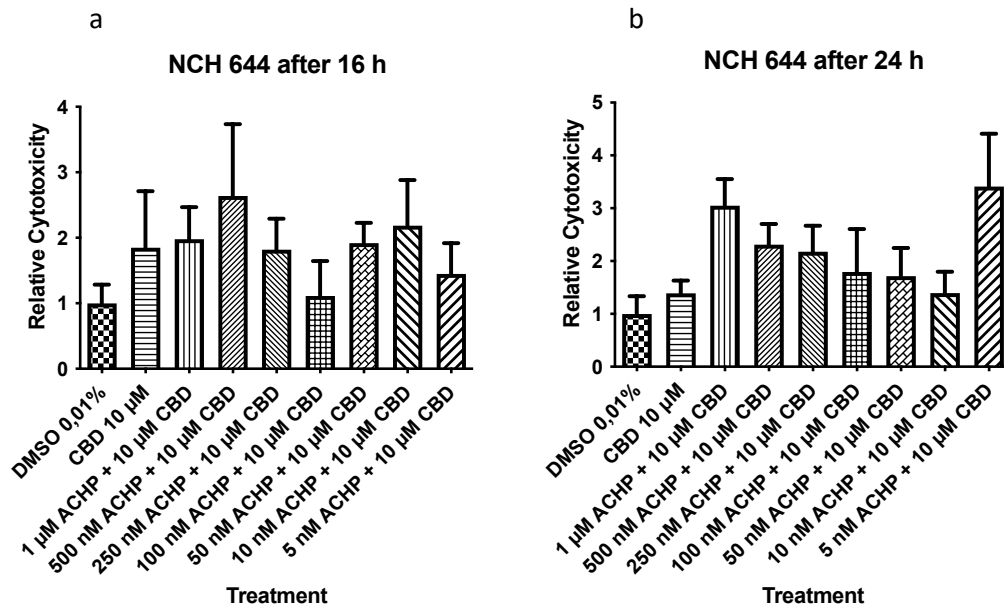


Figure 6: Relative cytotoxicity of CBD after pretreatment with ACHP in NCH 644. 3,000 cells of NCH 644 were seeded in each well. Each group consists of 5 biological replicates. 10 µM CBD were applied after pretreatment of 1 µM, 500 nM, 250 nM, 100 nM, 50 nM, 10 nM and 5 nM ACHP for 6 h, vehicle control was performed with DMSO 0.01%. Cytotoxicity was determined by TECAN® reader after (a) 16 h and (b) 24 h. The graph demonstrates that neither at 16 h nor at 24 h pretreatment with ACHP prevents or decreases the cytotoxic effect of CBD on NCH 644.

Results

8.2 Inhibition of the Translocation of NF- κ B with sn50

Although ACHP could not abrogate the cytotoxic effect of CBD, the approach was not completely rejected and another attempt was made to inhibit the translocation of NF- κ B elsewhere. For this purpose, the inhibitor NF- κ B sn50 was selected. NF- κ B sn50 is a small cell membrane-permeable peptide that carries both the nuclear localization sequence (NLS) of NF- κ B p50 and a hydrophobic region (h-region) and thus can inhibit the translocation of active NF- κ B complexes to the nucleus.

8.2.1 Cytotoxicity Assay

First, it was again examined whether NF- κ B sn50, at a dose that has been targeted in other work (Kolenko et al 1999, Lin et al 1995), has a cytotoxic effect on GBM cells on its own, or not. In the three cell lines NCH 644, Line 2, and Line 11, the vehicle control with DMSO 0.01% was compared with the groups with the inhibitor at the concentrations of 40 μ M, 20 μ M, 10 μ M, and 5 μ M NF- κ B sn50. As can be seen in Figures 7, 8 and 9, this showed no significant increase in relative cytotoxicity when comparing the control group with the different doses of NF- κ B sn50.

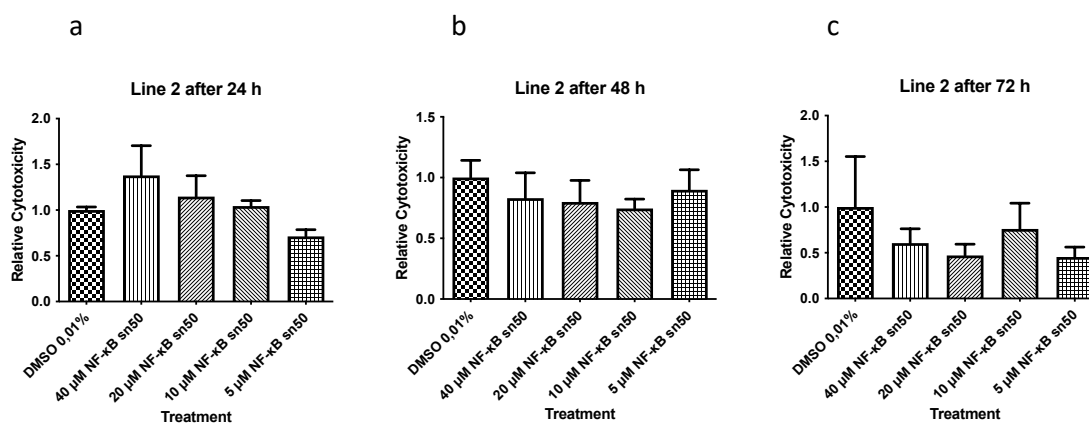


Figure 7: Relative cytotoxicity of NF- κ B sn50 in Line 2. 3,000 cells of Line 2 were seeded in each well. Each group consists of 5 biological replicates. NF- κ B sn50 was applied in 40 μ M, 20 μ M, 10 μ M and 5 μ M doses, vehicle control with DMSO 0.01%. Cytotoxicity was determined by TECAN® reader after (a) 24 h, (b) 48 h and (c) 72 h. The graphs display that at no time a significant difference in relative cytotoxicity in comparison with the control group occurred, which negates a direct cytotoxic effect of NF- κ B sn50 on Line 2.

Results

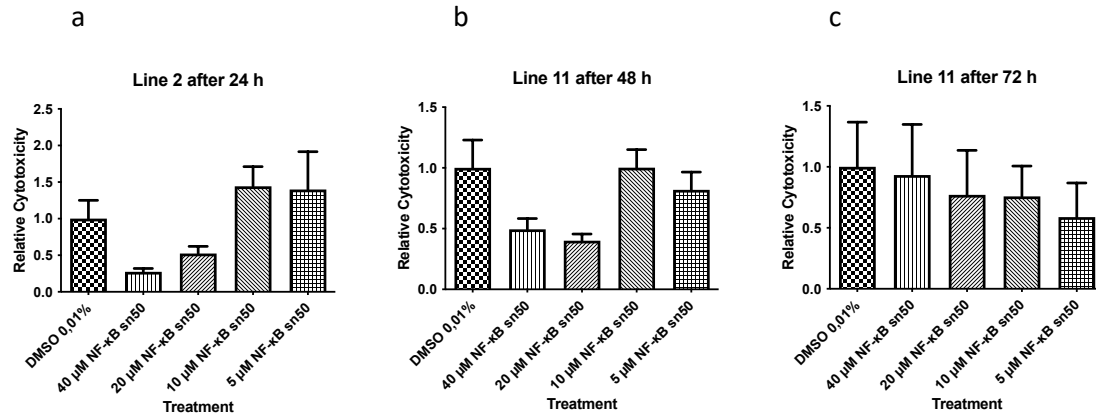


Figure 8: Relative cytotoxicity of NF- κ B sn50 in Line 11. 3,000 cells of Line 11 were seeded in each well. Each group consists of 5 biological replicates. NF- κ B sn50 was applied in 40 μ M, 20 μ M, 10 μ M and 5 μ M doses, vehicle control with DMSO 0.01%. Cytotoxicity was determined by TECAN® reader after (a) 24 h, (b) 48 h and (c) 72 h. The graphs display that at no time a significant increase in relative cytotoxicity in comparison with the control group occurred, which negates a direct cytotoxic effect of NF- κ B sn50 on Line 11.

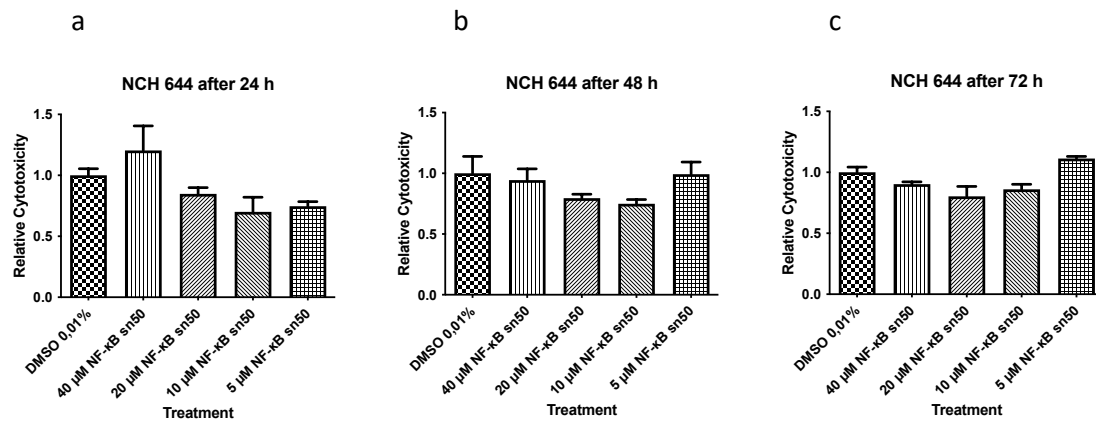


Figure 9: Relative cytotoxicity of NF- κ B sn50 in NCH 644. 3,000 cells of NCH 644 were seeded in each well. Each group consists of 5 biological replicates. NF- κ B sn50 was applied in 40 μ M, 20 μ M, 10 μ M and 5 μ M doses, vehicle control with DMSO 0.01%. Cytotoxicity was determined by TECAN® reader after (a) 24 h, (b) 48 h and (c) 72 h. The graphs display that at no time a significant increase in relative cytotoxicity in comparison with the control group occurred, which negates a direct cytotoxic effect of NF- κ B sn50 on NCH 644.

Results

In the following, the interaction of NF- κ B sn50 and CBD was investigated. For this purpose, the three cell lines were each pretreated with the doses of 20 μ M, 10 μ M, or 5 μ M NF- κ B sn50 for 6 h before 10 μ M CBD was added. As it's demonstrated in Figure 10, 11 and 12, at 24 h after the addition of CBD, the groups that were pretreated with NF- κ B sn50 showed a significant reduction in relative cytotoxicity compared to the groups with CBD without the inhibitor. Similarly, there were no increases in relative cytotoxicity in the groups pretreated with NF- κ B sn50 compared with the control group with DMSO 0.01%, supporting the absence of the cytotoxic effect of CBD with inhibition of the NF- κ B pathway.

This cytotoxicity assay thus demonstrates that without sufficient translocation of NF- κ B to the nucleus, the cytotoxic effect of CBD is absent in CBD-responsive cells. This in turn suggests that translocation of NF- κ B into the nucleus is essential for the effect of CBD on GBM cells.

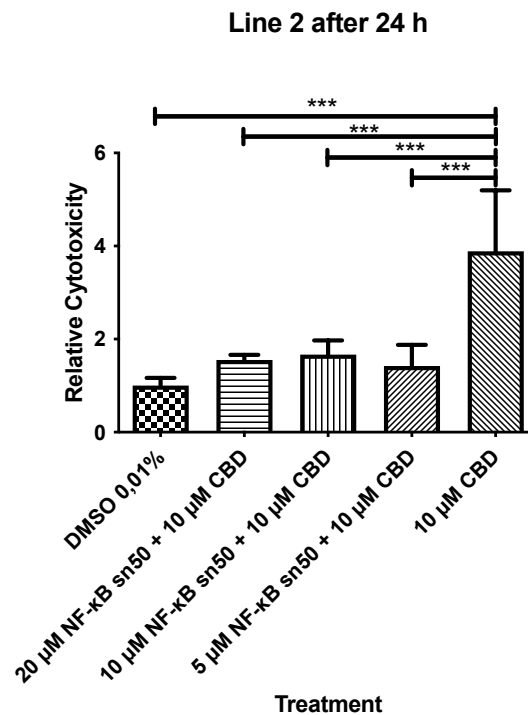


Figure 10: Relative cytotoxicity of CBD after pretreatment with NF- κ B sn50 in Line 2. 3,000 cells of Line 2 were seeded in each well. Each group consists of 5 biological replicates. 4 technical replicates were conducted ($n=4$). 20 μ M, 10 μ M or 5 μ M NF- κ B sn50 was applied 6 h prior to the 10 μ M CBD application. Vehicle control was performed with DMSO 0.01%. Cytotoxicity was determined by TECAN® reader 24 h after the CBD treatment. NF- κ B sn50 significantly reduced the cytotoxic effect of CBD in Line 2 ($p<0.001$).

Results

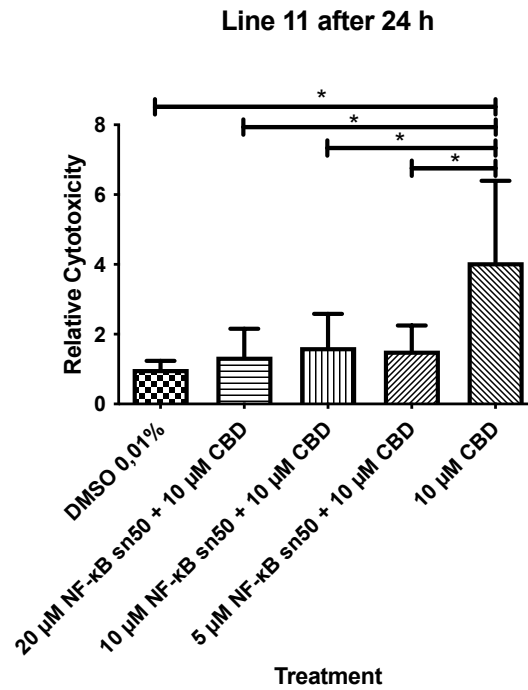


Figure 11: Relative cytotoxicity of CBD after pretreatment with NF-κB sn50 in Line 11. 3,000 cells of Line 11 were seeded in each well. Each group consists of 5 biological replicates. 4 technical replicates were conducted (n=4). 20 µM, 10 µM or 5 µM NF-κB sn50 was applied 6 h prior to the 10 µM CBD application. Vehicle control was performed with DMSO 0.01%. Cytotoxicity was determined by TECAN® reader 24 h after the CBD treatment. NF-κB sn50 significantly reduced the cytotoxic effect of CBD in Line 11 (p<0.05).

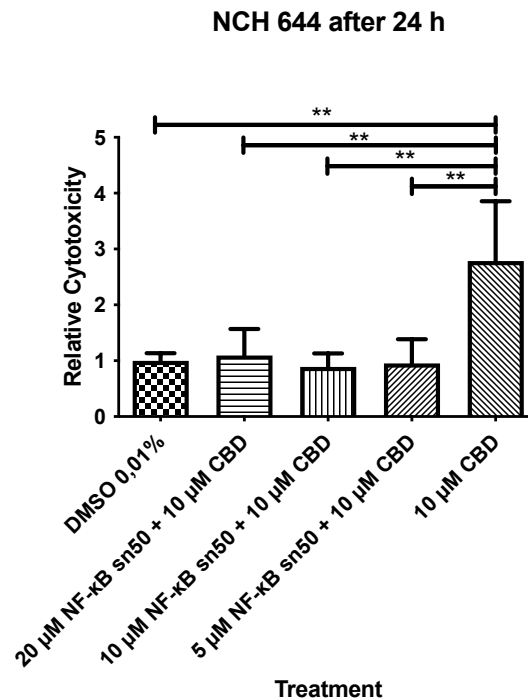


Figure 12: Relative cytotoxicity of CBD after pretreatment with NF-κB sn50 in NCH 644. 3,000 cells of NCH 644 were seeded in each well. Each group consists of 5 biological replicates. 4 technical replicates were conducted (n=4). 20 µM, 10 µM or 5 µM NF-κB sn50 was applied 6 h prior to the 10 µM CBD application. Vehicle control was performed with DMSO 0.01%. Cytotoxicity was determined by TECAN® reader 24 h after the CBD treatment. NF-κB sn50 significantly reduced the cytotoxic effect of CBD in NCH 644 (p<0.005).

Results

8.2.2 Immunocytochemistry

To better visualize the interaction of NF- κ B sn50 with the NF- κ B pathway, Immunocytochemistry fluorescence staining was added in a second part. This was intended to show that the inhibitor NF- κ B sn50 indeed inhibits the translocation of NF- κ B into the nucleus and that the effect of reducing cytotoxicity shown in the previous sections can therefore be attributed to this inhibition.

For this purpose, the cell lines NCH 644, Line 2 and Line 11 were incubated in chambered slides and then treated according to each of the groups mentioned. Thus, in addition to vehicle control with DMSO 0.01%, cells were treated with 10 μ M CBD, 10 μ M NF- κ B sn50, or 10 μ M NF- κ B sn50 for 6 h followed by 10 μ M CBD. As a positive control for pronounced translocation of NF- κ B p65 to the nucleus, one group was treated with 10 ng/ml TNF α for 1 h, as this causes rapid, although not long-lasting, but very pronounced nuclear translocation of NF- κ B p65 (Volmar et al 2021).

16 h after the addition of CBD, cells were fixed and stained with fluorescent antibody against NF- κ B p65 total. Nuclei were visualized with DAPI. The time point of 16 h after CBD addition was chosen because at this time NF- κ B p65 should already be reliably present in the nucleus of the cells without the cytotoxic effect already being so pronounced that most cells had already perished. Figure 13 (a), 14 (a) and 15 (a) show these stainings of the cell lines Line 2, Line 11, and NCH 644. In the vehicle control groups, it was clearly visible how most of the nuclei appeared to be excluded from the NF- κ B p65 total staining, indicating that there was far more NF- κ B p65 total in the cytosol than in the nucleus. The same was the case in the groups with NF- κ B sn50 alone. As expected, the cytosol remained strongly stained and most of the nuclei only weakly stained. The situation was different in the groups with 10 μ M CBD, in which most cells showed clear staining of the nuclei. This was comparable in intensity to the groups in which the expected strong staining of the nuclei by the previously applied TNF α had occurred. In the now decisive groups, in which the cells were first pretreated with NF- κ B sn50 for 6 h and subsequently exposed to the influence of CBD, a strong staining of the cytoplasm was seen with mostly simultaneous absence of staining of the nuclei. Since no absolute result was obtained in all groups, i.e., not all nuclei were either stained or not stained, the positively stained nuclei were counted and placed in relation to the total number of cells. The comparison of these ratios is shown in Figure 13 (b), 14 (b) and 15 (b). These quantitatively

Results

illustrate that not only is NF- κ B p65 total more frequently translocated into nuclei in the CBD groups, but also that this same translocation can be abrogated by application of NF- κ B sn50. This visualization of the inhibition of the translocation of NF- κ B p65 total in combination with the results from the cytotoxicity assay strengthen the assumption that NF- κ B p65 and its translocation into the nucleus is essential for the cytotoxic effect of CBD in CBD-sensitive GBM.

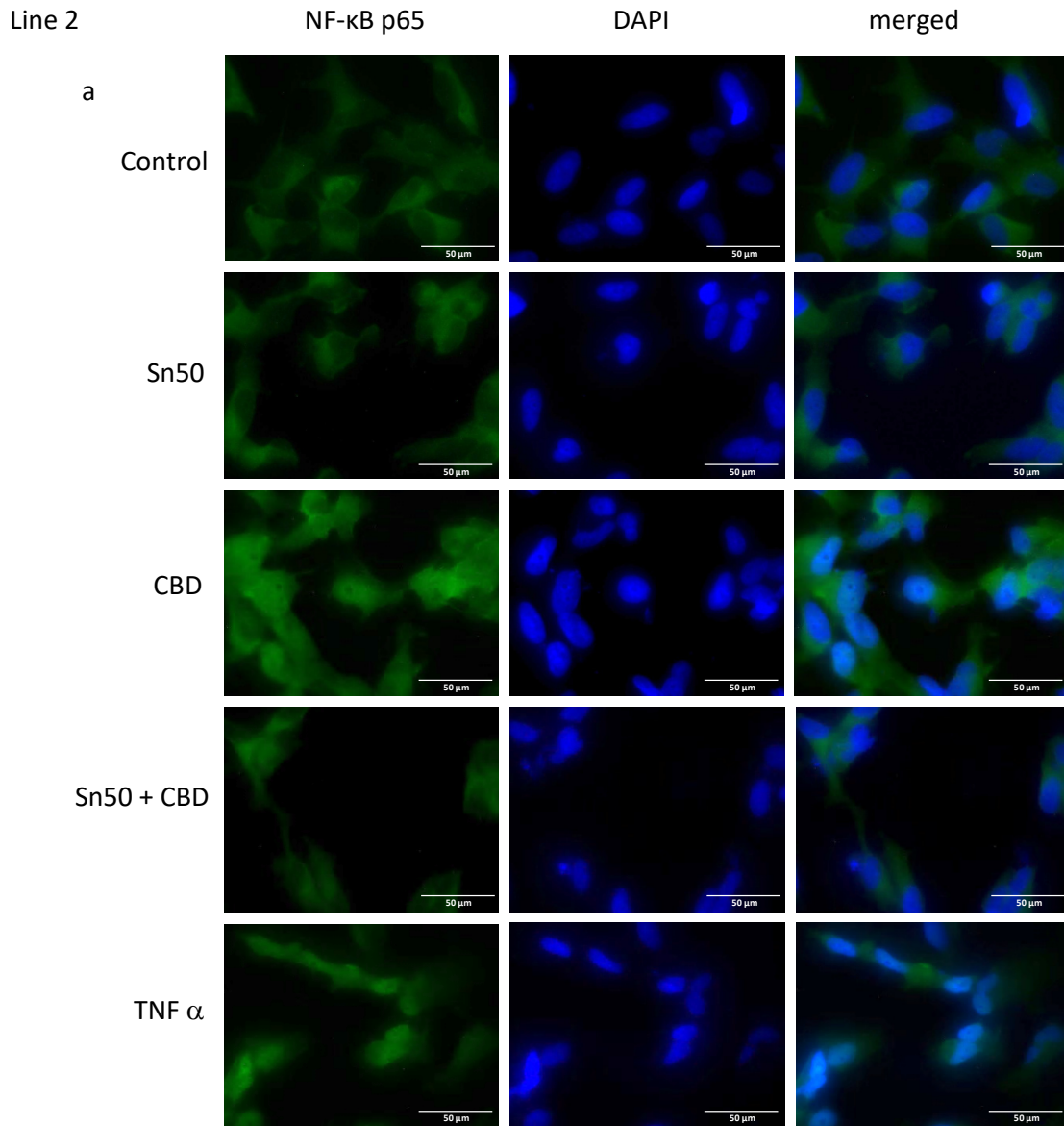


Figure 13: Immunocytochemistry of NF- κ B p65 in Line 2. a: fluorescence microscopy images show staining for NF- κ B p65 in Line 2 (40x magnification). Cells were incubated in chambered slides and treated with either the vehicle control DMSO 0.01%, 10 μ M NF- κ B sn50 only, 10 μ M CBD only, 10 μ M CBD after pretreatment with 10 μ M NF- κ B sn50 for 6 h, or 10 ng/ml TNF α for 1 h. CBD causes distinct translocation of NF- κ B p65 to the nucleus as measured after 16 h. TNF α causes a strong translocation of NF- κ B p65 to the nucleus after 1 h. NF- κ B sn50 markedly inhibits nuclear translocation of NF- κ B p65 and prevents the nuclear translocation of NF- κ B p65 induced by CBD. b: Comparison of the ratios of the positive stained nuclei of the groups mentioned in a. CBD causes significant translocation of NF- κ B p65 into the nucleus compared to vehicle control ($p < 0.001$). NF- κ B p65 sn50 causes significant inhibition of the CBD induced translocation of NF- κ B p65 into the nucleus ($p < 0.001$). $n = 5$

Results

Line 11

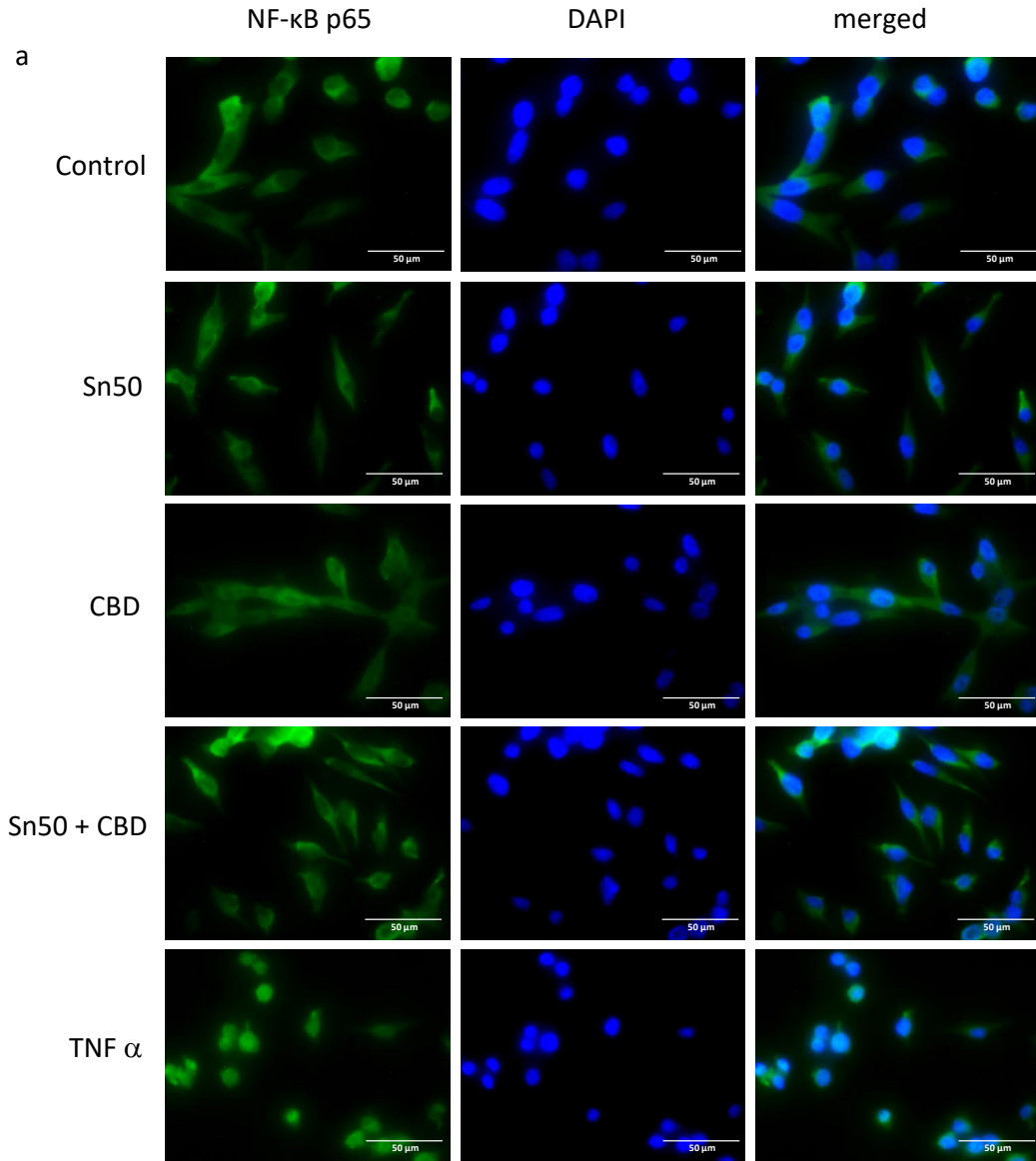
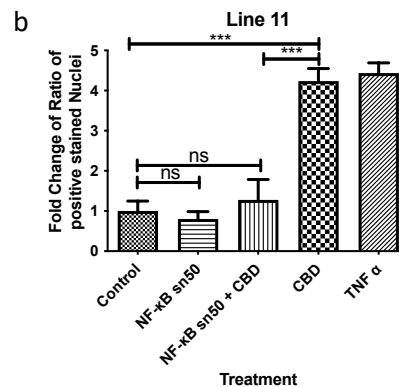


Figure 14: Immunocytochemistry of NF-κB p65 in Line 11. *a:* fluorescence microscopy images show staining for NF-κB p65 in Line 11 (40x magnification). Cells were incubated in chambered slides and treated with either the vehicle control DMSO 0.01%, 10 μM NF-κB sn50 only, 10 μM CBD only, 10 μM CBD after pretreatment with 10 μM NF-κB sn50 for 6 h, or 10 ng/ml TNF α for 1 h. CBD causes distinct translocation of NF-κB p65 to the nucleus as measured after 16 h. TNF α causes a strong translocation of NF-κB p65 to the nucleus after 1 h. NF-κB sn50 markedly inhibits nuclear translocation of NF-κB p65 and prevents the nuclear translocation of NF-κB p65 induced by CBD. *b:* Comparison of the ratios of the positive stained nuclei of the groups mentioned in *a*. CBD causes significant translocation of NF-κB p65 into the nucleus compared to vehicle control ($p < 0.001$). NF-κB p65 sn50 causes significant inhibition of the CBD induced translocation of NF-κB p65 into the nucleus ($p < 0.001$). $n = 5$



Results

NCH 644

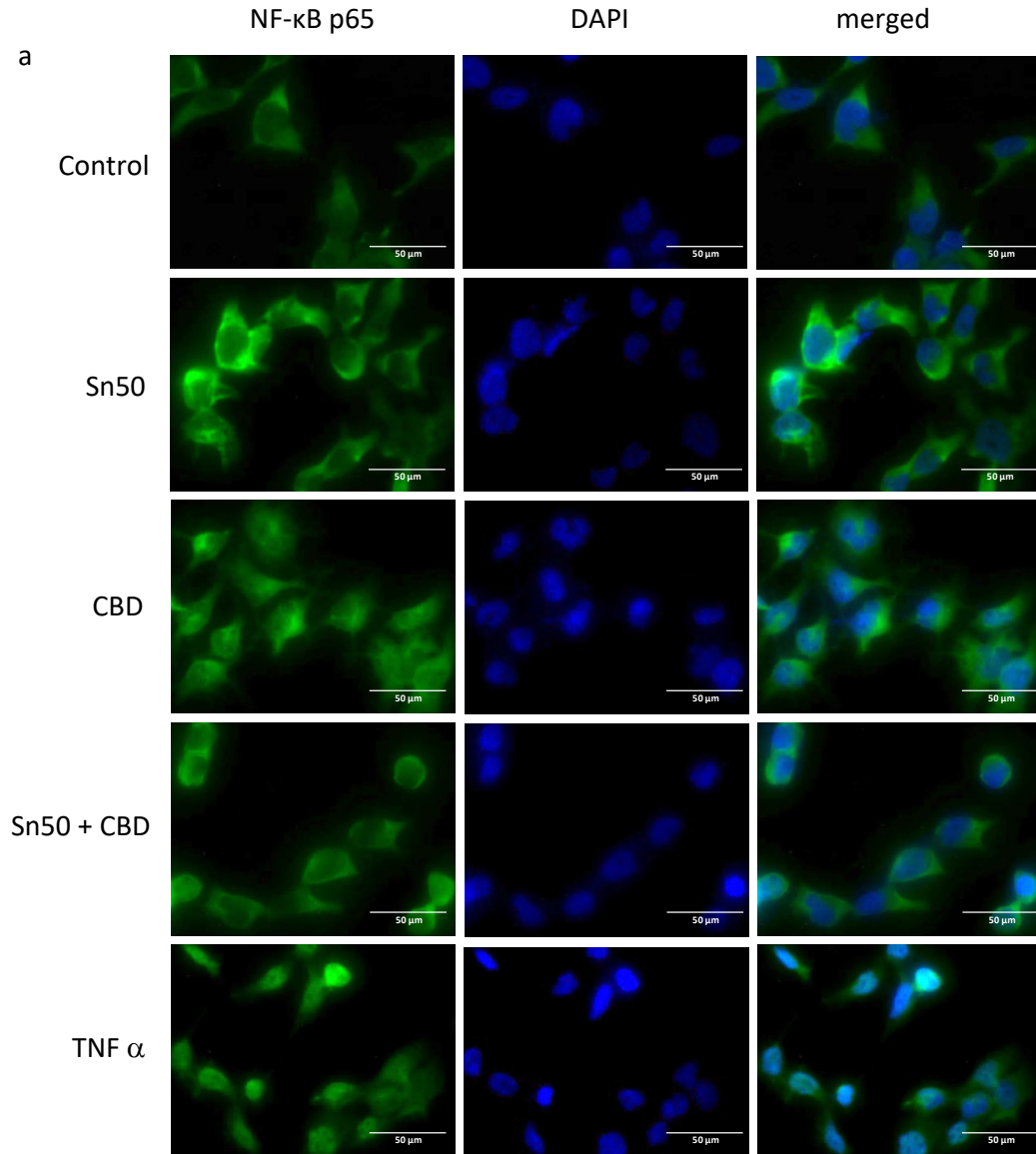
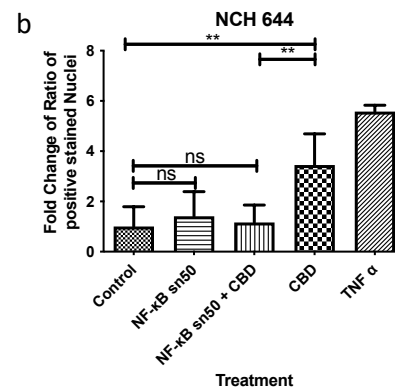


Figure 15: Immunocytochemistry of NF- κ B p65 in NCH 644. a: fluorescence microscopy images show staining for NF- κ B p65 in NCH 644 (40x magnification). Cells were incubated in chambered slides and treated with either the vehicle control DMSO 0.01%, 10 μ M NF- κ B sn50 only, 10 μ M CBD only, 10 μ M CBD after pretreatment with 10 μ M NF- κ B sn50 for 6 h, or 10 ng/ml TNF α for 1 h. CBD causes distinct translocation of NF- κ B p65 to the nucleus as measured after 16 h. TNF α causes a strong translocation of NF- κ B p65 to the nucleus after 1 h. NF- κ B sn50 markedly inhibits nuclear translocation of NF- κ B p65 and prevents the nuclear translocation of NF- κ B p65 induced by CBD. b: Comparison of the ratios of the positive stained nuclei of the groups mentioned in a. CBD causes significant translocation of NF- κ B p65 into the nucleus compared to vehicle control ($p < 0.005$). NF- κ B p65 sn50 causes significant inhibition of the CBD induced translocation of NF- κ B p65 into the nucleus ($p < 0.005$). $n = 5$



Results

8.3 Role of PKC ζ in selected GBM Cell Lines

The second part of this work further evaluates the role of PKC ζ in GBM cells. As mentioned in the introduction, NF- κ B p65 phosphorylation of ser-311 is essential for NF- κ B to fulfill its proper function including cell survival. Since NF- κ B p65 phospho ser-311 could be detected in CBD responders (Alenezi 2022, Volmar et al 2021), this part focuses on the detection of PKC ζ in GBM cells.

8.3.1 MTT Assay

A PKC ζ pseudosubstrate was used for competitive inhibition of PKC ζ , which should reduce cell survival due to the absence of NF- κ B p65 phosphorylation at Ser-311. Therefore, the PKC ζ pseudosubstrate was employed to indirectly demonstrate the presence of PKC ζ in GBM cell lines. Even though the cytotoxicity assay was the first choice of measuring the cytotoxic effect of the agent, it did not function adequately to detect the effect of the PKC ζ pseudosubstrate on GBM cells. Therefore, the cell viability assay (MTT assay) was utilized.

A total of 6 GBM cell lines were tested, including 4 GBM cell lines of human origin, Line 2, Line 11, NCH 644 and GBM 20, and 2 murine GBM cell lines, p53172H-PDGFB and cdkn2aKO-EGFRvIII. Cells were treated with PKC ζ pseudosubstrate at concentrations of 25 μ M, 10 μ M, or 5 μ M for 24 h. Similarly, in addition to the control group treated with DMSO 0.01%, one group each was treated with 10 μ M CBD for 24 to display the known cytotoxic effect of CBD in the MTT assay. The measurements showed, as can be seen in Figure 16 to 21, that significantly fewer cells had survived in the groups treated with the PKC ζ pseudosubstrate compared to the control group. Especially in the groups with the higher concentration, the number of still viable cells was strongly decreased. This gives evidence that PKC zeta is present in GBM cell lines and that its inhibition is associated with an expected decreased cell survival.

Results

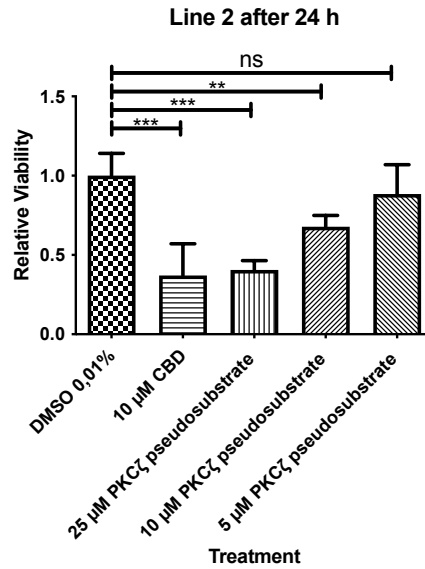


Figure 16: Relative viability of Line 2 after PKC ζ pseudosubstrate-treatment. 3,000 cells of Line 2 were seeded in each well. Each group consists of 3 biological replicates. 5 technical replicates were conducted ($n=5$). 25 μM , 10 μM or 5 μM PKC ζ pseudosubstrate were applied, vehicle control was performed with DMSO 0.01%. Measuring with ELISA reader after 24 h. The graph shows a significantly reduced cell viability in the groups treated with 25 μM ($p<0.001$) and 10 μM PKC ζ pseudosubstrate ($p<0.005$). Hence, inhibition of PKC ζ results in a decreased cell survival.

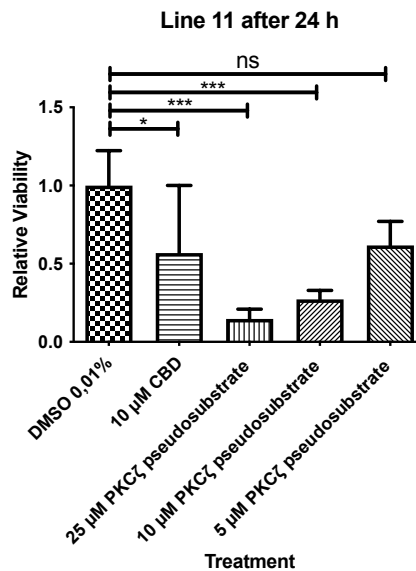


Figure 17: Relative viability of Line 11 after PKC ζ pseudosubstrate-treatment. 3,000 cells of Line 11 were seeded in each well. Each group consists of 3 biological replicates. 5 technical replicates were conducted ($n=5$). 25 μM , 10 μM or 5 μM PKC ζ pseudosubstrate were applied, vehicle control was performed with DMSO 0.01%. Measuring with ELISA reader after 24 h. The graph shows a significantly reduced cell viability in the groups treated with 25 μM , 10 μM PKC ζ pseudosubstrate ($p<0.001$). Hence, inhibition of PKC ζ results in a decreased cell survival.

Results

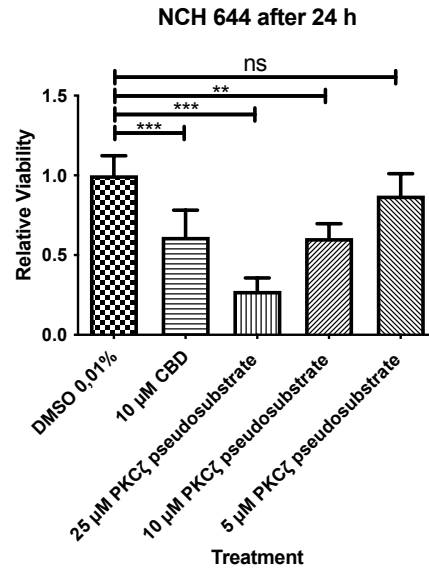


Figure 18: Relative viability of NCH 644 after PKC ζ pseudosubstrate-treatment. 3,000 cells of NCH 644 were seeded in each well. Each group consists of 3 biological replicates. 5 technical replicates were conducted ($n=5$). 25 μM , 10 μM or 5 μM PKC ζ pseudosubstrate were applied, vehicle control was performed with DMSO 0.01%. Measuring with ELISA reader after 24 h. The graph shows a significantly reduced cell viability in the groups treated with 25 μM ($p<0.001$) and 10 μM PKC ζ pseudosubstrate ($p<0.005$). Hence, inhibition of PKC ζ results in a decreased cell survival.

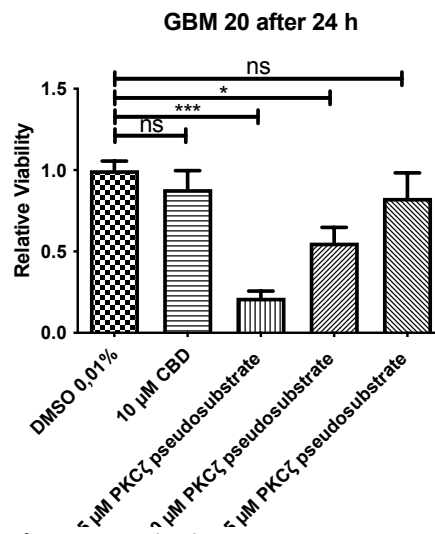


Figure 19: Relative viability of GBM 20 after PKC ζ pseudosubstrate-treatment. 3,000 cells of GBM 20 were seeded in each well. Each group consists of 3 biological replicates. 5 technical replicates were conducted ($n=5$). 25 μM , 10 μM or 5 μM PKC ζ pseudosubstrate were applied, vehicle control was performed with DMSO 0.01%. Measuring with ELISA reader after 24 h. The graph shows a significantly reduced cell viability in the groups treated with 25 μM ($p<0.001$) and 10 μM PKC ζ pseudosubstrate ($p<0.05$). Hence, inhibition of PKC ζ results in a decreased cell survival.

Results

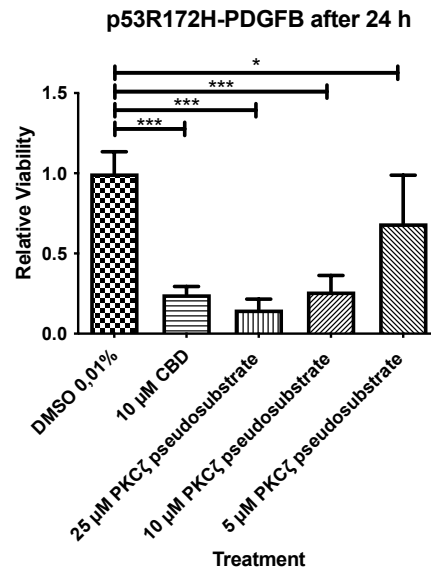


Figure 20: Relative viability of p53172H-PDGFB after PKC ζ pseudosubstrate-treatment. 3,000 cells of p53172H-PDGFB were seeded in each well. Each group consists of 3 biological replicates. 5 technical replicates were conducted (n=5). 25 μ M, 10 μ M or 5 μ M PKC ζ pseudosubstrate were applied, vehicle control was performed with DMSO 0.01%. Measuring with ELISA reader after 24 h. The graph shows a significantly reduced cell viability in the groups treated with 25 μ M, 10 μ M ($p < 0.001$) and 5 μ M PKC ζ pseudosubstrate ($p < 0.05$). Hence, inhibition of PKC ζ results in a decreased cell survival.

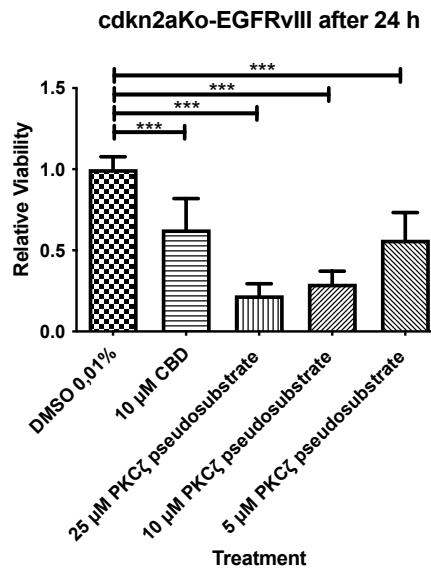


Figure 21: Relative viability of cdkn2aKo-EGFRvIII after PKC ζ pseudosubstrate-treatment. 3,000 cells of Line 2 were seeded in each well. Each group consists of 3 biological replicates. 5 technical replicates were conducted (n=5). 25 μ M, 10 μ M or 5 μ M PKC ζ pseudosubstrate were applied, vehicle control was performed with DMSO 0.01%. Measuring with ELISA reader after 24 h. The graph shows a significantly reduced cell viability in the groups treated with 25 μ M, 10 μ M and 5 μ M PKC ζ pseudosubstrate ($p < 0.001$). Hence, inhibition of PKC ζ results in a decreased cell survival.

Results

8.3.2 Immunocytochemistry

To investigate the CBD triggered cell death pathway in more detail, PKC ζ was additionally stained by immunocytochemistry. Therefore, in total 6 GBM cell lines were utilized, 3 CBD-sensitive cell lines, Line 2, Line 11 and NCH 644, and 3 CBD-non-sensitive cell lines, NCH 441, NCH 421k and GBM 14. Cells were incubated in chamber slides and either treated with 16 μ M CBD or the vehicle control DMSO 0.01%. Again, the fixation took place after 16 h and staining was performed using anti-PKC ζ -antibody. Here, PKC ζ was found to be present in both CBD-sensitive and CBD-non-sensitive cell lines. Comparing the images of each cell line in terms of CBD treatment results were varying (Figure 22 to 27). In Line 2 and Line 11, the amount of PKC ζ detectable remained equally between the two groups. In NCH 644, a slightly more pronounced signal from the PKC ζ staining was apparent after CBD treatment. In NCH 441 and NCH 421k, a clearly attenuated intensity of PKC ζ signaling was detectable after CBD treatment. In GBM 14 the PKC ζ signal remained equally.

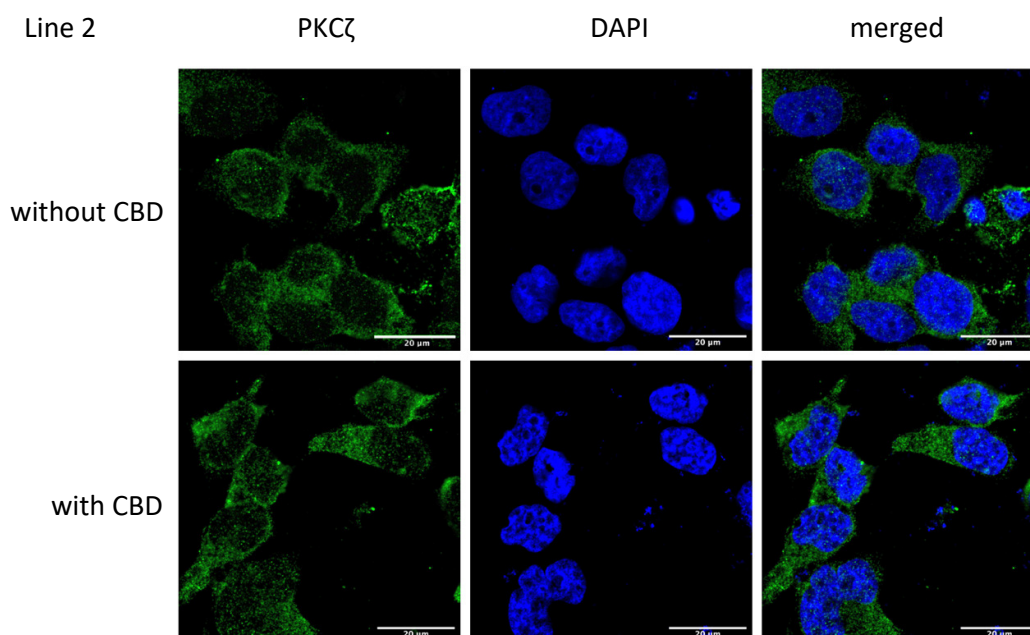


Figure 22: Confocal microscopy of Line 2 with fluorescent staining of PKC ζ without and with CBD treatment (40x magnification). Cells were incubated in chambered slides and either treated with the vehicle control DMSO 0.01% or with 10 μ M CBD for 16 h. Both groups display a predominantly cytoplasmic distribution of PKC ζ . CBD did not induce any alterations in the expression level of PKC ζ .

Results

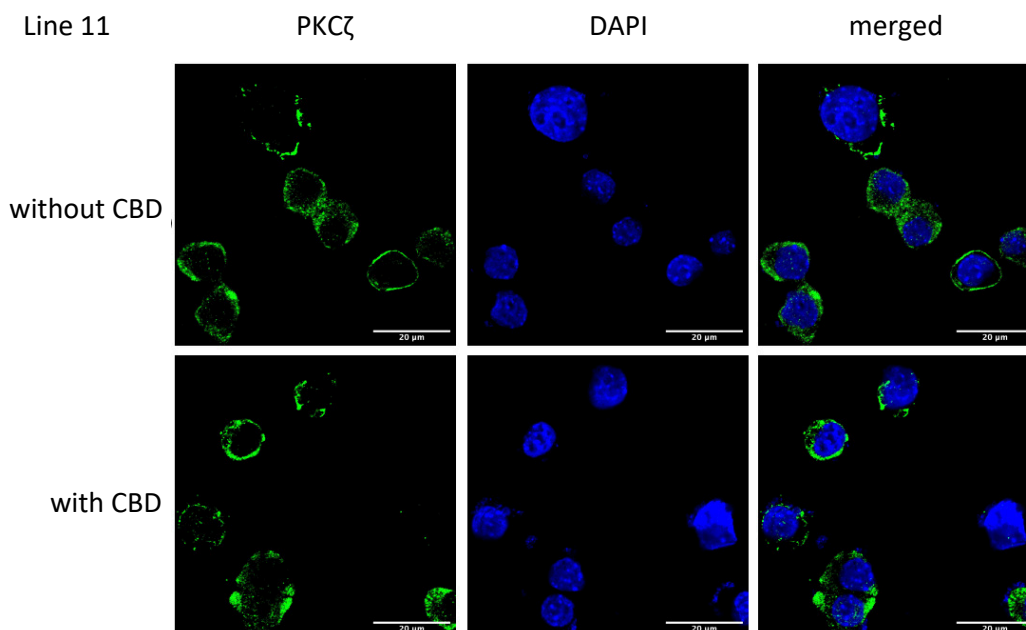


Figure 23: Confocal microscopy of Line 11 with fluorescent staining of PKC ζ without and with CBD treatment (40x magnification). Cells were incubated in chambered slides and either treated with the vehicle control DMSO 0.01% or with 10 μ M CBD for 16 h. Both groups display a predominantly cytoplasmic distribution of PKC ζ . CBD did not induce any alterations in the expression level of PKC ζ .

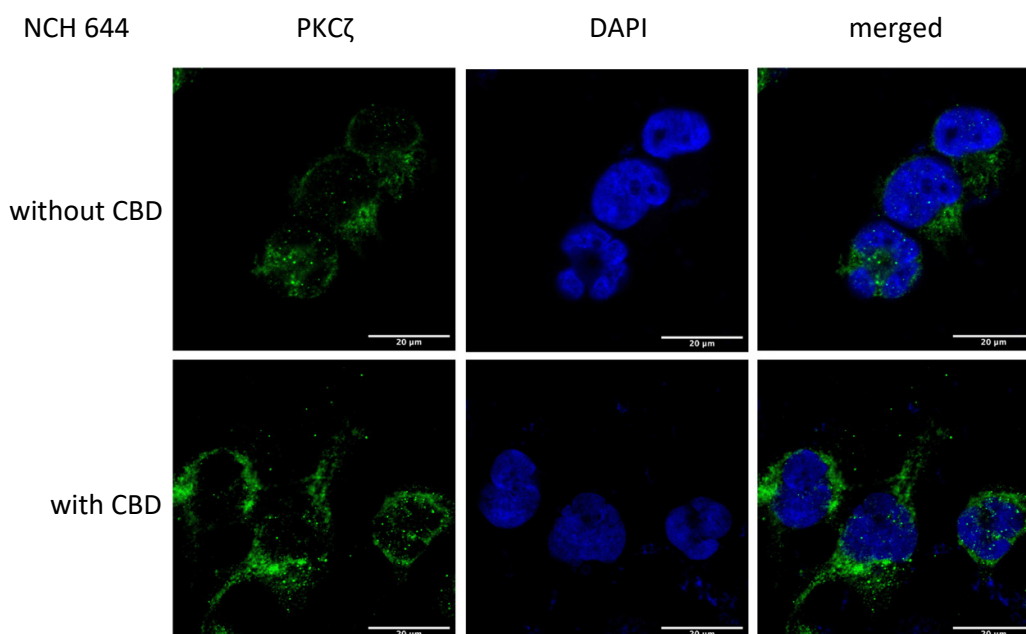


Figure 24: Confocal microscopy of NCH 644 with fluorescent staining of PKC ζ without and with CBD treatment (40x magnification). Cells were incubated in chambered slides and either treated with the vehicle control DMSO 0.01% or with 10 μ M CBD for 16 h. Both groups display a predominantly cytoplasmic distribution of PKC ζ . CBD causes a slightly increased PKC ζ signal.

Results

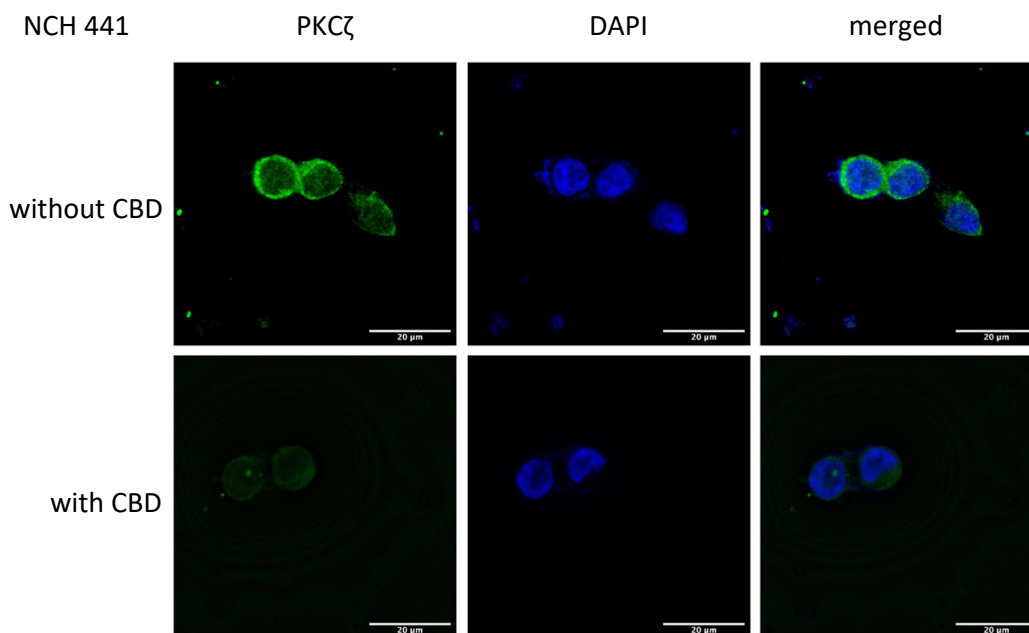


Figure 25: Confocal microscopy of NCH 441 with fluorescent staining of PKC ζ without and with CBD treatment (40x magnification). Cells were incubated in chambered slides and either treated with the vehicle control DMSO 0.01% or with 10 μ M CBD for 16 h. Both groups display a predominantly cytoplasmic distribution of PKC ζ . In cells treated with CBD, the level of PKC ζ is markedly decreased.

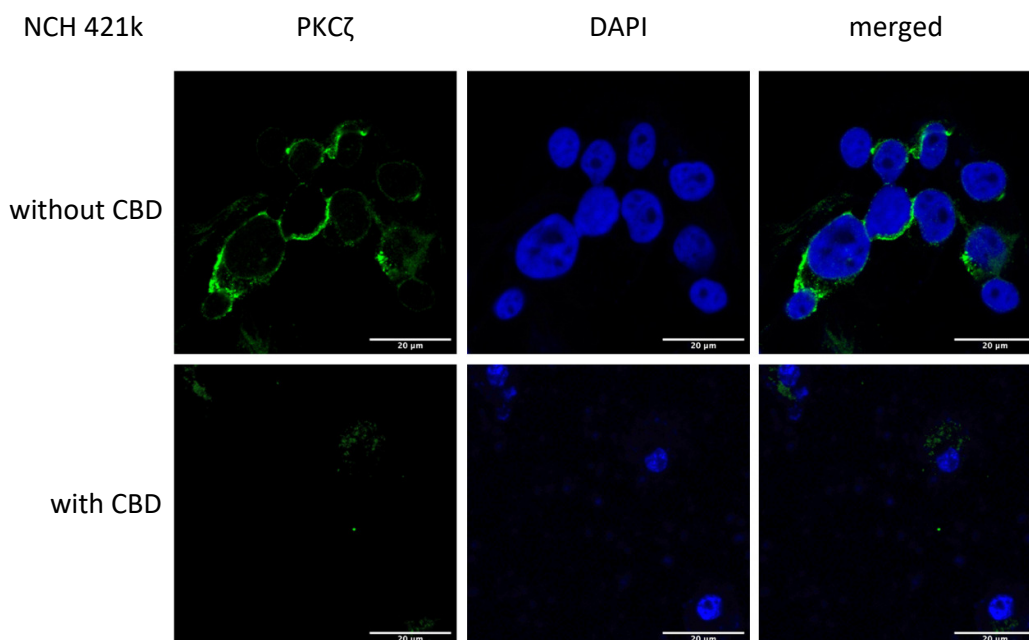


Figure 26: Confocal microscopy of NCH 421k with fluorescent staining of PKC ζ without and with CBD treatment (40x magnification). Cells were incubated in chambered slides and either treated with the vehicle control DMSO 0.01% or with 10 μ M CBD for 16 h. Both groups display a predominantly cytoplasmic distribution of PKC ζ . In cells treated with CBD, the level of PKC ζ is markedly decreased.

Results

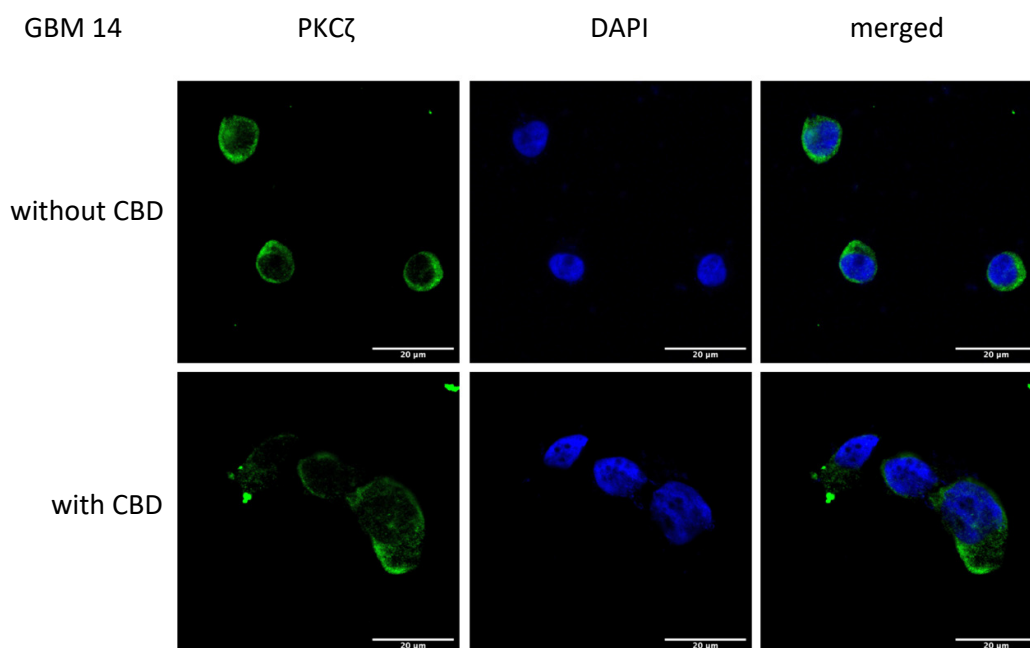


Figure 27: Confocal microscopy of GBM 14 with fluorescent staining of PKC ζ without and with CBD treatment (40x magnification). Cells were incubated in chambered slides and either treated with the vehicle control DMSO 0.01% or with 10 μ M CBD for 16 h. Both groups display a predominantly cytoplasmic distribution of PKC ζ . CBD did not induce any alterations in the expression level of PKC ζ .

9 Discussion

The transcription factor NF- κ B is important for cell survival and proliferation. Dysregulated NF- κ B can be observed in many different tumor types, including GBM (Dolcet et al 2005, Volmar et al 2021). NF- κ B has garnered attention as a promising target for therapies aimed at inhibiting and modulating its activity. However, interfering with the NF- κ B pathway presents challenges. NF- κ B is ubiquitously expressed in all human cells to a greater or lesser extent. Interfering with the signaling pathway can thus lead to undesired adverse effects in any cell or organ system (Donovan et al 2017, Gupta et al 2010). Thus, although inhibition of the NF- κ B pathway has been shown to be associated with improved response to chemotherapeutic agents and radiation in some tumor entities (Mortezaee et al 2019), it should not be neglected that NF- κ B is crucial for many more physiological aspects. For instance, considering NF- κ Bs function in the immune system (Zeligs et al 2016). NF- κ B is implicated in both tumor-promoting and tumor-depressing activities (Perkins 2004). Beside promoting proliferation in tumor cells itself, NF- κ B stimulates the production of cytokines by immune cells outside the tumor microenvironment, which are pro-inflammatory and stimulating for the tumor-promoting NF- κ B pathway of tumor cells (Zeligs et al 2016). On the other hand, however, activation of the classical NF- κ B pathway promotes the expression of Major Histocompatibility Complex Class I-related Chain A gene (MICA), which encodes a protein that is a target for natural killer (NK) cells (Molinero et al 2004). Furthermore, activation of the classical pathway promotes differentiation of T cells into Th17 cells, which are thought to play a role in anti-tumor immunity (Zeligs et al 2016). These few examples illustrate why specific modulation of the NF- κ B pathway is necessary.

9.1 Interpretation of the Results of the Inhibition of the Translocation of NF- κ B

CBD has a cytotoxic effect on certain GBM cells (Nagl 2022). Likewise, CBD had been shown to induce increased translocation of NF- κ B p65. However, in this nuclear translocation of NF- κ B p65 initiated by CBD, it is observed that phosphorylation of NF- κ B p65 at ser-311, unlike translocation induced by other substances such as TNF alpha, is absent (Alenezi 2022, Volmar et al 2021). Until now, it was not clear whether this translocation of NF- κ B to the nucleus was crucial for the cytotoxic effect of CBD. This question was addressed in the first part of this work using the inhibitor NF- κ B sn50. The cytotoxicity assay thereby indicated that the additional pretreatment of the cells with NF- κ B sn50 prevented the cytotoxic effect of CBD. In

Discussion

addition, immunocytochemical staining was performed, which gave evidence that in those GBM cells in which the cytotoxic effect of CBD was absent due to the pretreatment with NF- κ B sn50, no translocation of NF- κ B p65 into the nucleus induced by CBD could be achieved due to the inhibitor. Taken together, these two findings indicate that translocation of NF- κ B p65 into the nucleus, which is induced by CBD, is crucial for the cytotoxic effect of CBD.

This would also explain why the combination of TNF α with CBD has an enhanced and more rapid onset of cytotoxic effect than CBD on its own. TNF α provides rapid translocation of NF- κ B into the nucleus, accelerating the accumulation of NF- κ B p65 with absent phosphorylation at ser-311, which is required for the cytotoxic effect of CBD in CBD-sensitive cells (Alenezi 2022, Nagl 2022)

9.2 Interpretation of the Results of the Investigations on PKC ζ

Previous studies in our research facility have revealed changes in post-translational modification under the influence of CBD. In particular, it has been induced that in CBD-sensitive cells phosphorylation at ser-311 is absent under CBD (Volmar et al 2021). An enzyme that can carry out this phosphorylation under physiological conditions is PKC ζ (Duran 2003). Suppression of this phosphorylation of NF- κ B p65 at ser-311 results in NF- κ B p65 being able to bind to the appropriate sites on DNA, but its transcriptional activity is significantly reduced (Levy et al 2011). It is precisely this mechanism that was targeted in the second part of this work to investigate whether PKC ζ is present in GBM cells in which the cytotoxic effect of CBD could be induced. The results demonstrate that inhibition of PKC ζ by a pseudosubstrate was associated with reduced cell survival. Thus, it can be assumed that PKC ζ is present in the GBM cell lines studied. In addition, immunocytochemistry staining was performed to visually depict and semiquantitatively analyze the distribution of PKC ζ before and after CBD treatment. On the one hand, it could be confirmed that PKC ζ is present in CBD-sensitive, but also in non-CBD-sensitive, GBM cells. This, in combination with the previous results, suggests that PKC ζ is present in GBM cells and that influencing its activity has a direct impact on cell survival of GBM cells. This, in turn, raises the possibility of whether CBD affects PKC ζ activity or expression. Whether the expression of PKC ζ was affected by CBD was also assessed in the stainings. However, in the immunocytochemical stainings, a consistent change in the distribution pattern or intensity following treatment with CBD was not observed in either the CBD-sensitive or the non-CBD-sensitive cell group.

Discussion

Two of three CBD-sensitive cells, Line 2 and Line 11, did not display any changes in PKC ζ expression, whereas one cell line, NCH 644, did display an increased amount of PKC ζ after CBD treatment. However, if one were to assume that the decreased cell survival after CBD treatment is dependent on less NF- κ B p65 being phosphorylated by PKC ζ at ser-311, this observation is less fitting into the overall picture.

In contrast, two out of three of the non-CBD-sensitive GBM cell lines induced a decrease in expression of PKC ζ after CBD treatment. However, no decrease in the amount of NF- κ B p65 phosphorylated at ser-311 could be detected in these non-CBD-sensitive cells in another work (Alenezi 2022, Volmar et al 2021). Similarly, in this work, CBD was observed to downregulate Prkcz, the gene encoding PKC ζ (Volmar et al 2021).

One possible aspect that may be crucial for the interaction between PKC ζ and NF- κ B p65 is localization. PKC ζ is predominantly localized in the cytoplasm (Kiley & Parker 1995), as confirmed by immunocytochemical staining. The phosphorylation of NF- κ B p65 at ser-311 by PKC ζ occurs primarily in the nucleus, after PKC ζ was activated and translocated into the nucleus (Umar 2000, Yao et al 2010). Nonetheless, there are indications of alternative intracellular localizations of PKC ζ . For instance, there is evidence that PKC ζ can also be membrane-localized (Muscella A 2005). Though, a membrane-localized PKC ζ , might have little effect on the phosphorylation of NF- κ B p65 unless there are additional proteins that facilitate the intracellular transport of NF- κ B p65 to the membraneous PKC ζ prior to the nuclear translocation. Currently (as of 2025), there is no evidence of such a protein. It should be noted that while the immunocytochemical stainings conducted in this study provide an initial visual assessment of cellular localization, additional methods such as Western blotting should be employed to accurately distinguish between cytoplasmic, nuclear, and membraneous fractions.

Eventually, the role of PKC ζ needs to be further illuminated. In the experiments 16 h after CBD treatment was set as the optimal time in terms of fixation and subsequently staining. Adhering to this time interval had proven appropriate for assessing whether and to what extent translocation of NF- κ B p65 into the nucleus had occurred after CBD treatment (Alenezi 2022). Nevertheless, it might be not optimal fitting for the PKC ζ staining. It is possible that a different time point might be more appropriate for this. However, immunocytochemistry may not be the optimal method to evaluate the expression of PKC ζ in response to CBD.

Discussion

In addition, the PKC ζ enzyme activity was not further investigated in the experiments in this work as well as in those at our research facility. These could also contribute a partial component to the observed effect of decreased phosphorylation of NF- κ B p65.

9.3 Prospect for the future of CBD on Glioblastoma

The results of our research group have shown that CBD indeed has a cytotoxic effect on CBD-sensitive GBM cells in vitro and in mouse experiments (Volmar et al 2021). In this regard, a crucial part of this cytotoxic effect can be attributed to the translocation of NF- κ B p65 into the nucleus, which, however, is not phosphorylated at ser-311. The absence of this phosphorylation can be attributed to PKC ζ , which is involved in the signaling pathway of CBD. This can be due in part to the downregulation of gene expression of Prkcz (Volmar et al 2021). Although the signaling pathway was elucidated in major points, some mechanisms remain uncertain.

In the meantime, further publications have demonstrated an anti-tumor effect of cannabinoids on GBM cells. CBD was also shown to be a cannabinoid with a great anti-tumor effect, but combinations with additional THC treatment have also been shown to be beneficial. The majority of all work on cannabinoids and GBM relates to preclinical trials utilizing in-vitro cell culturing or in-vivo experiments with mouse models (Kyriakou et al 2021, Lopez-Valero et al 2018). The few first approaches with cannabinoids in patients with GBM are currently not surpassing Phase I or II (Schloss et al 2021, Twelves et al 2021).

CBD has been proven to be a well tolerated agent with its success in other neurological disorders. Epidyolex[®] is approved by the EMA for the treatment of Dravet-syndrome or Lennox-Gastaut-syndrome in children (ema.europa.eu 2021). Nabiximol, a combined preparation of CBD and THC, is utilized in the treatment of spasticity in MS patients (Collin et al 2007).

The side effect profile of CBD is favorable and severe adverse effects are rare, when used by its own or in combination with other drugs, e.g., antiepileptics. Nevertheless, CBD-drug interactions shall not be underestimated since CBD is interacting with several enzymes of the cytochrome P450 family (Huestis et al 2019, Ibeas Bih et al 2015). This is especially important since CBD can be obtained prescription free. This characteristic of a drug can mislead to the assumption that the drug does not cause any adverse effects or interactions with other drugs

Discussion

at all. In addition, one should always keep in mind that the quality and purity of CBD production beyond certified suppliers can be considered questionable (Lachenmeier et al 2021).

Thus, to further evaluate the role of CBD in the treatment of GBM, more extensive studies in GBM patients are needed. Furthermore, the determination of subtypes and their response to a possible CBD treatment could be purposeful in identifying patients who may benefit from it. This could be integrated in patients who are undergoing neurosurgery anyway and in whom a sample is obtained for pathology. This could pave the way for CBD as an optional add-on therapy in patients with GBM.

Bibliography

10 Bibliography

- Adams R, Hunt M, Clark JH. 1940. Structure of Cannabidiol, a Product Isolated from the Marihuana Extract of Minnesota Wild Hemp. I. *Journal of the American Chemical Society* 62: 196-200
- Ahrens J, Demir R, Leuwer M, De La Roche J, Krampfl K, et al. 2009. The Nonpsychotropic Cannabinoid Cannabidiol Modulates and Directly Activates Alpha-1 and Alpha-1-Beta Glycine Receptor Function. *Pharmacology* 83: 217-22
- Aldape K, Brindle KM, Chesler L, Chopra R, Gajjar A, et al. 2019. Challenges to curing primary brain tumours. *Nature Reviews Clinical Oncology* 16: 509-20
- Aldape KD, Ballman K, Furth A, Buckner JC, Giannini C, et al. 2004. Immunohistochemical detection of EGFRvIII in high malignancy grade astrocytomas and evaluation of prognostic significance. *J Neuropathol Exp Neurol* 63: 700-7
- Alenezi H. 2022. Investigating the effect of cannabidiol on NF- κ B phosphorylation and nuclear translocation in glioblastoma cells.
- Anrather J, Csizmadia V, Soares MP, Winkler H. 1999. Regulation of NF- κ B RelA Phosphorylation and Transcriptional Activity by p21 and Protein Kinase C ζ in Primary Endothelial Cells. *Journal of Biological Chemistry* 274: 13594-603
- Arenzana-Seisdedos F, Turpin P, Rodriguez M, Thomas D, Hay RT, et al. 1997. Nuclear localization of I kappa B alpha promotes active transport of NF-kappa B from the nucleus to the cytoplasm. *Journal of Cell Science* 110: 369-78
- Bisogno T, Hanuš L, De Petrocellis L, Tchilibon S, Ponde DE, et al. 2001. Molecular targets for cannabidiol and its synthetic analogues: effect on vanilloid VR1 receptors and on the cellular uptake and enzymatic hydrolysis of anandamide. *British Journal of Pharmacology* 134: 845-52
- Blessing EM, Steenkamp MM, Manzanares J, Marmar CR. 2015. Cannabidiol as a Potential Treatment for Anxiety Disorders. *Neurotherapeutics* 12: 825-36
- Bonizzi G, Karin M. 2004. The two NF-kappaB activation pathways and their role in innate and adaptive immunity. *Trends Immunol* 25: 280-8
- Brennan CW, Verhaak RG, McKenna A, Campos B, Noushmehr H, et al. 2013. The somatic genomic landscape of glioblastoma. *Cell* 155: 462-77
- Burstein S. 2015. Cannabidiol (CBD) and its analogs: a review of their effects on inflammation. *Bioorg Med Chem* 23: 1377-85
- Campos AC, Moreira FA, Gomes FV, Del Bel EA, Guimarães FS. 2012. Multiple mechanisms involved in the large-spectrum therapeutic potential of cannabidiol in psychiatric disorders. *Philosophical Transactions of the Royal Society B: Biological Sciences* 367: 3364-78
- Chakravarti A, Zhai G, Suzuki Y, Sarkesh S, Black PM, et al. 2004. The prognostic significance of phosphatidylinositol 3-kinase pathway activation in human gliomas. *J Clin Oncol* 22: 1926-33
- Christian F, Smith E, Carmody R. 2016. The Regulation of NF- κ B Subunits by Phosphorylation. *Cells* 5: 12
- Collin C, Davies P, Mutiboko IK, Ratcliffe S, Sativex Spasticity in MSSG. 2007. Randomized controlled trial of cannabis-based medicine in spasticity caused by multiple sclerosis. *Eur J Neurol* 14: 290-6
- De Petrocellis L, Vellani V, Schiano-Moriello A, Marini P, Magherini PC, et al. 2008. Plant-derived cannabinoids modulate the activity of transient receptor potential channels of ankyrin type-1 and melastatin type-8. *J Pharmacol Exp Ther* 325: 1007-15

Bibliography

- Devane WA, Hanus L, Breuer A, Pertwee RG, Stevenson LA, et al. 1992. Isolation and structure of a brain constituent that binds to the cannabinoid receptor. *Science* 258: 1946-9
- Devinsky O, Cross JH, Laux L, Marsh E, Miller I, et al. 2017. Trial of Cannabidiol for Drug-Resistant Seizures in the Dravet Syndrome. *New England Journal of Medicine* 376: 2011-20
- Devinsky O, Marsh E, Friedman D, Thiele E, Laux L, et al. 2016. Cannabidiol in patients with treatment-resistant epilepsy: an open-label interventional trial. *Lancet Neurol* 15: 270-8
- Devinsky O, Patel AD, Cross JH, Villanueva V, Wirrell EC, et al. 2018. Effect of Cannabidiol on Drop Seizures in the Lennox–Gastaut Syndrome. *New England Journal of Medicine* 378: 1888-97
- Dobrzanski P, Ryseck RP, Bravo R. 1993. Both N- and C-terminal domains of RelB are required for full transactivation: role of the N-terminal leucine zipper-like motif. *Mol Cell Biol* 13: 1572-82
- Dolcet X, Llobet D, Pallares J, Matias-Guiu X. 2005. NF- κ B in development and progression of human cancer. *Virchows Archiv* 446: 475-82
- Donovan JM, Zimmer M, Offman E, Grant T, Jirousek M. 2017. A Novel NF- κ B Inhibitor, Edasalonexent (CAT-1004), in Development as a Disease-Modifying Treatment for Patients With Duchenne Muscular Dystrophy: Phase 1 Safety, Pharmacokinetics, and Pharmacodynamics in Adult Subjects. *The Journal of Clinical Pharmacology* 57: 627-39
- Donson AM, Banerjee A, Gamboni-Robertson F, Fleitz JM, Foreman NK. 2000. Protein kinase C zeta isoform is critical for proliferation in human glioblastoma cell lines. *Journal of Neuro-Oncology* 47: 109-15
- Duran A. 2003. Essential role of RelA Ser311 phosphorylation by PKC in NF- κ B transcriptional activation. *The EMBO Journal* 22: 3910-18
- Eljamel MS, Mahboob SO. 2016. The effectiveness and cost-effectiveness of intraoperative imaging in high-grade glioma resection; a comparative review of intraoperative ALA, fluorescein, ultrasound and MRI. *Photodiagnosis Photodyn Ther* 16: 35-43
- Eriksson M, Kahari J, Vestman A, Hallmans M, Johansson M, et al. 2019. Improved treatment of glioblastoma - changes in survival over two decades at a single regional Centre. *Acta Oncol* 58: 334-41
- Funakoshi Y, Hata N, Takigawa K, Arita H, Kuga D, et al. 2021. Clinical significance of *CDKN2A* homozygous deletion in combination with methylated *MGMT* status for *IDH* -wildtype glioblastoma. *Cancer Medicine* 10: 3177-87
- Gai Q-J, Fu Z, He J, Mao M, Yao X-X, et al. 2022. EPHA2 mediates PDGFA activity and functions together with PDGFRA as prognostic marker and therapeutic target in glioblastoma. *Signal Transduction and Targeted Therapy* 7
- Gerondakis S, Grossmann M, Nakamura Y, Pohl T, Grumont R. 1999. Genetic approaches in mice to understand Rel/NF- κ B and I κ B function: transgenics and knockouts. *Oncogene* 18: 6888-95
- Ghovanloo M-R, Shuart NG, Mezeyova J, Dean RA, Ruben PC, Goodchild SJ. 2018. Inhibitory effects of cannabidiol on voltage-dependent sodium currents. *Journal of Biological Chemistry* 293: 16546-58
- Gil J, Peters G. 2006. Regulation of the INK4b–ARF–INK4a tumour suppressor locus: all for one or one for all. *Nature Reviews Molecular Cell Biology* 7: 667-77

Bibliography

- Gilbert MR, Dignam JJ, Armstrong TS, Wefel JS, Blumenthal DT, et al. 2014. A Randomized Trial of Bevacizumab for Newly Diagnosed Glioblastoma. *New England Journal of Medicine* 370: 699-708
- Guérit E, Arts F, Dachy G, Boulouadnine B, Demoulin J-B. 2021. PDGF receptor mutations in human diseases. *Cellular and Molecular Life Sciences* 78: 3867-81
- Guo G, Gong K, Wohlfeld B, Hatanpaa KJ, Zhao D, Habib AA. 2015. Ligand-Independent EGFR Signaling. *Cancer Research* 75: 3436-41
- Gupta SC, Sundaram C, Reuter S, Aggarwal BB. 2010. Inhibiting NF- κ B activation by small molecules as a therapeutic strategy. *Biochimica et Biophysica Acta (BBA) - Gene Regulatory Mechanisms* 1799: 775-87
- Han S, Liu Y, Cai SJ, Qian M, Ding J, et al. 2020. IDH mutation in glioma: molecular mechanisms and potential therapeutic targets. *British Journal of Cancer* 122: 1580-89
- Hanna C, Lawrie TA, Rogozińska E, Kernohan A, Jefferies S, et al. 2020. Treatment of newly diagnosed glioblastoma in the elderly: a network meta-analysis. *Cochrane Database of Systematic Reviews* 2020
- Hayden MS, Ghosh S. 2004. Signaling to NF- κ B. *Genes & Development* 18: 2195-224
- Hayden MS, Ghosh S. 2012. NF- κ B, the first quarter-century: remarkable progress and outstanding questions. *Genes & Development* 26: 203-34
- Hegi ME, Diserens AC, Gorlia T, Hamou MF, de Tribolet N, et al. 2005. MGMT gene silencing and benefit from temozolomide in glioblastoma. *N Engl J Med* 352: 997-1003
- Heusch M, Lin L, Geleziunas R, Greene WC. 1999. The generation of nfkb2 p52: mechanism and efficiency. *Oncogene* 18: 6201-8
- Hindocha C, Freeman TP, Schafer G, Gardener C, Das RK, et al. 2015. Acute effects of delta-9-tetrahydrocannabinol, cannabidiol and their combination on facial emotion recognition: a randomised, double-blind, placebo-controlled study in cannabis users. *Eur Neuropsychopharmacol* 25: 325-34
- Hochrainer K, Racchumi G, Anrather J. 2013. Site-specific Phosphorylation of the p65 Protein Subunit Mediates Selective Gene Expression by Differential NF- κ B and RNA Polymerase II Promoter Recruitment. *Journal of Biological Chemistry* 288: 285-93
- Houston DB, Howlett AC. 1993. Solubilization of the cannabinoid receptor from rat brain and its functional interaction with guanine nucleotide-binding proteins. *Mol Pharmacol* 43: 17-22
- Howlett AC. 2002. The cannabinoid receptors. *Prostaglandins Other Lipid Mediat* 68-69: 619-31
- Huber MA, Denk A, Peter RU, Weber L, Kraut N, Wirth T. 2002. The IKK-2/I κ B α /NF- κ B Pathway Plays a Key Role in the Regulation of CCR3 and eotaxin-1 in Fibroblasts. *Journal of Biological Chemistry* 277: 1268-75
- Huestis MA, Gorelick DA, Heishman SJ, Preston KL, Nelson RA, et al. 2001. Blockade of Effects of Smoked Marijuana by the CB1-Selective Cannabinoid Receptor Antagonist SR141716. *Archives of General Psychiatry* 58: 322
- Huestis MA, Solimini R, Pichini S, Pacifici R, Carlier J, Busardò FP. 2019. Cannabidiol Adverse Effects and Toxicity. *Current Neuropharmacology* 17: 974-89
- Huet O, Petit JM, Ratinaud MH, Julien R. 1992. NADH-dependent dehydrogenase activity estimation by flow cytometric analysis of 3-(4,5-dimethylthiazolyl-2-yl)-2,5-diphenyltetrazolium bromide (MTT) reduction. *Cytometry* 13: 532-39
- Huxford T, Huang D-B, Malek S, Ghosh G. 1998. The Crystal Structure of the I κ B α /NF- κ B Complex Reveals Mechanisms of NF- κ B Inactivation. *Cell* 95: 759-70

Bibliography

- Ibeas Bih C, Chen T, Nunn AVW, Bazelat M, Dallas M, Whalley BJ. 2015. Molecular Targets of Cannabidiol in Neurological Disorders. *Neurotherapeutics* 12: 699-730
- Iffland K, Grotenhermen F. 2017. An Update on Safety and Side Effects of Cannabidiol: A Review of Clinical Data and Relevant Animal Studies. *Cannabis and Cannabinoid Research* 2: 139-54
- Jacobs MD, Harrison SC. 1998. Structure of an I κ B α /NF- κ B Complex. *Cell* 95: 749-58
- Jankowska S, Lewandowska M, Masztalewicz M, Sagan L, Nowacki P, Urasińska E. 2021. Molecular classification of glioblastoma based on immunohistochemical expression of EGFR, PDGFRA, NF1, IDH1, p53 and PTEN proteins. *Polish Journal of Pathology* 72: 1-10
- Jenkinson MD, Barone DG, Bryant A, Vale L, Bulbeck H, et al. 2018. Intraoperative imaging technology to maximise extent of resection for glioma. *Cochrane Database of Systematic Reviews* 2021
- Kang JH, Toita R, Kim CW, Katayama Y. 2012. Protein kinase C (PKC) isozyme-specific substrates and their design. *Biotechnol Adv* 30: 1662-72
- Kiley SC, Parker PJ. 1995. Differential localization of protein kinase C isozymes in U937 cells: evidence for distinct isozyme functions during monocyte differentiation. *Journal of Cell Science* 108: 1003-16
- Kolenko V, Bloom T, Rayman P, Bukowski R, Hsi E, Finke J. 1999. Inhibition of NF-kappa B activity in human T lymphocytes induces caspase-dependent apoptosis without detectable activation of caspase-1 and -3. *J Immunol* 163: 590-8
- Kyriakou I, Yarandi N, Polycarpou E. 2021. Efficacy of cannabinoids against glioblastoma multiforme: A systematic review. *Phytomedicine* 88: 153533
- Lachenmeier DW, Habel S, Fischer B, Herbi F, Zerbe Y, et al. 2021. Are adverse effects of cannabidiol (CBD) products caused by tetrahydrocannabinol (THC) contamination? *F1000Research* 8: 1394
- Lallena M-J, Diaz-Meco MT, Bren G, Payá CV, Moscat J. 1999. Activation of I κ B Kinase β by Protein Kinase C Isoforms. *Molecular and Cellular Biology* 19: 2180-88
- Le Rhun E, Preusser M, Roth P, Reardon DA, Van Den Bent M, et al. 2019. Molecular targeted therapy of glioblastoma. *Cancer Treatment Reviews* 80: 101896
- Levy D, Kuo AJ, Chang Y, Schaefer U, Kitson C, et al. 2011. Lysine methylation of the NF- κ B subunit RelA by SETD6 couples activity of the histone methyltransferase GLP at chromatin to tonic repression of NF- κ B signaling. *Nature Immunology* 12: 29-36
- Li CC, Dai RM, Longo DL. 1995. Inactivation of NF-kappa B inhibitor I kappa B alpha: ubiquitin-dependent proteolysis and its degradation product. *Biochem Biophys Res Commun* 215: 292-301
- Liao G, Zhang M, Harhaj EW, Sun S-C. 2004. Regulation of the NF- κ B-inducing Kinase by Tumor Necrosis Factor Receptor-associated Factor 3-induced Degradation. *Journal of Biological Chemistry* 279: 26243-50
- Lin Y-Z, Yao S, Veach RA, Torgerson TR, Hawiger J. 1995. Inhibition of Nuclear Translocation of Transcription Factor NF- κ B by a Synthetic Peptide Containing a Cell Membrane-permeable Motif and Nuclear Localization Sequence. *Journal of Biological Chemistry* 270: 14255-58
- Ling L, Cao Z, Goeddel DV. 1998. NF- κ B-inducing kinase activates IKK- α by phosphorylation of Ser-176. *Proceedings of the National Academy of Sciences* 95: 3792-97
- Liu S-Y, Mei W-Z, Lin Z-X. 2013. Pre-Operative Peritumoral Edema and Survival Rate in Glioblastoma Multiforme. *Oncology Research and Treatment* 36: 679-84

Bibliography

- Lopez-Valero I, Saiz-Ladera C, Torres S, Hernandez-Tiedra S, Garcia-Taboada E, et al. 2018. Targeting Glioma Initiating Cells with A combined therapy of cannabinoids and temozolomide. *Biochem Pharmacol* 157: 266-74
- Louis DN, Perry A, Wesseling P, Brat DJ, Cree IA, et al. 2021. The 2021 WHO Classification of Tumors of the Central Nervous System: a summary. *Neuro Oncol* 23: 1231-51
- Louis DN, Wesseling P, Aldape K, Brat DJ, Capper D, et al. 2020. cIMPACT-NOW update 6: new entity and diagnostic principle recommendations of the cIMPACT-Utrecht meeting on future CNS tumor classification and grading. *Brain Pathol* 30: 844-56
- Mahgoub M, Keun-Hang SY, Sydorenko V, Ashoor A, Kabbani N, et al. 2013. Effects of cannabidiol on the function of alpha7-nicotinic acetylcholine receptors. *Eur J Pharmacol* 720: 310-9
- Malek S, Chen Y, Huxford T, Ghosh G. 2001. I κ B β , but Not I κ B α , Functions as a Classical Cytoplasmic Inhibitor of NF- κ B Dimers by Masking Both NF- κ B Nuclear Localization Sequences in Resting Cells. *Journal of Biological Chemistry* 276: 45225-35
- Mao X-G, Xue X-Y, Wang L, Lin W, Zhang X. 2022. Deep learning identified glioblastoma subtypes based on internal genomic expression ranks. *BMC Cancer* 22
- May MJ, D'Acquisto F, Madge LA, Glockner J, Pober JS, Ghosh S. 2000. Selective inhibition of NF-kappaB activation by a peptide that blocks the interaction of NEMO with the I κ B kinase complex. *Science* 289: 1550-4
- McGuire P, Robson P, Cubala WJ, Vasile D, Morrison PD, et al. 2018. Cannabidiol (CBD) as an Adjunctive Therapy in Schizophrenia: A Multicenter Randomized Controlled Trial. *American Journal of Psychiatry* 175: 225-31
- McKinnon C, Nandhabalan M, Murray SA, Plaha P. 2021. Glioblastoma: clinical presentation, diagnosis, and management. *BMJ*: n1560
- Mechoulam R, Ben-Shabat S, Hanus L, Ligumsky M, Kaminski NE, et al. 1995. Identification of an endogenous 2-monoglyceride, present in canine gut, that binds to cannabinoid receptors. *Biochem Pharmacol* 50: 83-90
- Mia MM, Bank RA. 2015. The I κ B kinase inhibitor AICP strongly attenuates TGF β 1-induced myofibroblast formation and collagen synthesis. *Journal of Cellular and Molecular Medicine* 19: 2780-92
- Miranzadeh Mahabadi H, Bhatti H, Laprairie RB, Taghibiglou C. 2021. Cannabinoid receptors distribution in mouse cortical plasma membrane compartments. *Molecular Brain* 14
- Molinero LL, Fuertes MB, Girart MV, Fainboim L, Rabinovich GA, et al. 2004. NF- κ B Regulates Expression of the MHC Class I-Related Chain A Gene in Activated T Lymphocytes. *The Journal of Immunology* 173: 5583-90
- Moorthy AK, Savinova OV, Ho JQ, Wang VY-F, Vu D, Ghosh G. 2006. The 20S proteasome processes NF- κ B1 p105 into p50 in a translation-independent manner. *The EMBO Journal* 25: 1945-56
- Mortezaee K, Najafi M, Farhood B, Ahmadi A, Shabeeb D, Musa AE. 2019. NF-kappaB targeting for overcoming tumor resistance and normal tissues toxicity. *J Cell Physiol* 234: 17187-204
- Munro S, Thomas KL, Abu-Shaar M. 1993. Molecular characterization of a peripheral receptor for cannabinoids. *Nature* 365: 61-65
- Muscella A SC, Marsigliante S. 2005. Atypical PKC-zeta and PKC-iota mediate opposing effects on MCF-7 Na⁺/K⁺ATPase activity. *Cell Physiol* 205: 278-85
- Mussbacher M, Salzmann M, Brostjan C, Hoesel B, Schoergenhofer C, et al. 2019. Cell Type-Specific Roles of NF-kappaB Linking Inflammation and Thrombosis. *Front Immunol* 10: 85

Bibliography

- Nagl B. 2022. Cannabinoide als mögliche Therapeutika für Glioblastome : TRPV-vermittelte Pharmakologie körpereigener Tumorabwehr.
- Naumann M, Nieters A, Hatada EN, Scheidereit C. 1993. NF-kappa B precursor p100 inhibits nuclear translocation and DNA binding of NF-kappa B/rel-factors. *Oncogene* 8: 2275-81
- Niles AL, Moravec RA, Eric Hesselberth P, Scurria MA, Daily WJ, Riss TL. 2007. A homogeneous assay to measure live and dead cells in the same sample by detecting different protease markers. *Anal Biochem* 366: 197-206
- O'Shea JM, Perkins ND. 2010. Thr435 phosphorylation regulates RelA (p65) NF-kappaB subunit transactivation. *Biochem J* 426: 345-54
- Oeckinghaus A, Ghosh S. 2009. The NF- B Family of Transcription Factors and Its Regulation. *Cold Spring Harbor Perspectives in Biology* 1: a000034-a34
- Ostrom QT, Gittleman H, Truitt G, Boscia A, Kruchko C, Barnholtz-Sloan JS. 2018. CBTRUS Statistical Report: Primary Brain and Other Central Nervous System Tumors Diagnosed in the United States in 2011-2015. *Neuro Oncol* 20: iv1-iv86
- Pahl HL. 1999. Activators and target genes of Rel/NF-kappaB transcription factors. *Oncogene* 18: 6853-66
- Pasparakis M, Luedde T, Schmidt-Suppran M. 2006. Dissection of the NF-kB signalling cascade in transgenic and knockout mice. *Cell Death & Differentiation* 13: 861-72
- Perkins ND. 2004. NF-kappaB: tumor promoter or suppressor? *Trends Cell Biol* 14: 64-9
- Perkins ND. 2006. Post-translational modifications regulating the activity and function of the nuclear factor kappa B pathway. *Oncogene* 25: 6717-30
- Philpott C, Tovell H, Frayling IM, Cooper DN, Upadhyaya M. 2017. The NF1 somatic mutational landscape in sporadic human cancers. *Human Genomics* 11
- Radwan MM, Chandra S, Gul S, Elsohly MA. 2021. Cannabinoids, Phenolics, Terpenes and Alkaloids of Cannabis. *Molecules* 26: 2774
- Rice NR, MacKichan ML, Israel A. 1992. The precursor of NF-kappa B p50 has I kappa B-like functions. *Cell* 71: 243-53
- Rimessi A, Patergnani S, Ioannidi E, Pinton P. 2013. Chemoresistance and Cancer-Related Inflammation: Two Hallmarks of Cancer Connected by an Atypical Link, PKCzeta. *Front Oncol* 3: 232
- Riva N, Mora G, Soraru G, Lunetta C, Ferraro OE, et al. 2019. Safety and efficacy of nabiximols on spasticity symptoms in patients with motor neuron disease (CANALS): a multicentre, double-blind, randomised, placebo-controlled, phase 2 trial. *Lancet Neurol* 18: 155-64
- Rivera AL, Pelloski CE, Sulman E, Aldape K. 2008. Prognostic and predictive markers in glioma and other neuroepithelial tumors. *Curr Probl Cancer* 32: 97-123
- Roskoski R, Jr. 2014. The ErbB/HER family of protein-tyrosine kinases and cancer. *Pharmacol Res* 79: 34-74
- Ross HR, Napier I, Connor M. 2008. Inhibition of recombinant human T-type calcium channels by Delta9-tetrahydrocannabinol and cannabidiol. *J Biol Chem* 283: 16124-34
- Russo EB, Burnett A, Hall B, Parker KK. 2005. Agonistic properties of cannabidiol at 5-HT1a receptors. *Neurochem Res* 30: 1037-43
- Ryberg E, Larsson N, Sjögren S, Hjorth S, Hermansson NO, et al. 2007. The orphan receptor GPR55 is a novel cannabinoid receptor. *British Journal of Pharmacology* 152: 1092-101

Bibliography

- Ryo A, Suizu F, Yoshida Y, Perrem K, Liou Y-C, et al. 2003. Regulation of NF- κ B Signaling by Pin1-Dependent Prolyl Isomerization and Ubiquitin-Mediated Proteolysis of p65/RelA. *Molecular Cell* 12: 1413-26
- Sabatel H, Di Valentin E, Gloire G, Dequiedt F, Piette J, Habraken Y. 2012. Phosphorylation of p65(RelA) on Ser547 by ATM Represses NF- κ B-Dependent Transcription of Specific Genes after Genotoxic Stress. *PLoS ONE* 7: e38246
- Sakurai H, Chiba H, Miyoshi H, Sugita T, Toriumi W. 1999. I κ B Kinases Phosphorylate NF- κ B p65 Subunit on Serine 536 in the Transactivation Domain. *Journal of Biological Chemistry* 274: 30353-56
- Savkovic SD, Koutsouris A, Hecht G. 2003. PKC zeta participates in activation of inflammatory response induced by enteropathogenic E. coli. *Am J Physiol Cell Physiol* 285: C512-21
- Schloss J, Lacey J, Sinclair J, Steel A, Sughrue M, et al. 2021. A Phase 2 Randomised Clinical Trial Assessing the Tolerability of Two Different Ratios of Medicinal Cannabis in Patients With High Grade Gliomas. *Front Oncol* 11: 649555
- Schmitz ML, Baeuerle PA. 1991. The p65 subunit is responsible for the strong transcription activating potential of NF-kappa B. *The EMBO Journal* 10: 3805-17
- Sejda A, Grajkowska W, Trubicka J, Szutowicz E, Wojdacz T, et al. 2022. WHO CNS5 2021 classification of gliomas: a practical review and road signs for diagnosing pathologists and proper patho-clinical and neuro-oncological cooperation. *Folia Neuropathologica* 60: 137-52
- Sen R, Baltimore D. 1986a. Inducibility of kappa immunoglobulin enhancer-binding protein Nf-kappa B by a posttranslational mechanism. *Cell* 47: 921-8
- Sen R, Baltimore D. 1986b. Multiple nuclear factors interact with the immunoglobulin enhancer sequences. *Cell* 46: 705-16
- Senftleben U, Cao Y, Xiao G, Greten FR, Krahn G, et al. 2001. Activation by IKKalpha of a second, evolutionary conserved, NF-kappa B signaling pathway. *Science* 293: 1495-9
- Siebenlist U, Franzoso G, Brown K. 1994. Structure, Regulation and Function of NF-kappaB. *Annual Review of Cell Biology* 10: 405-55
- Songtao Q, Lei Y, Si G, Yanqing D, Huixia H, et al. 2012. IDH mutations predict longer survival and response to temozolomide in secondary glioblastoma. *Cancer Science* 103: 269-73
- Stupp R, Mason WP, Van Den Bent MJ, Weller M, Fisher B, et al. 2005. Radiotherapy plus Concomitant and Adjuvant Temozolomide for Glioblastoma. *New England Journal of Medicine* 352: 987-96
- Sun S-C. 2011. Non-canonical NF- κ B signaling pathway. *Cell Research* 21: 71-85
- Tachibana M, Ueda J, Fukuda M, Takeda N, Ohta T, et al. 2005. Histone methyltransferases G9a and GLP form heteromeric complexes and are both crucial for methylation of euchromatin at H3-K9. *Genes & Development* 19: 815-26
- Thomas A, Baillie GL, Phillips AM, Razdan RK, Ross RA, Pertwee RG. 2007. Cannabidiol displays unexpectedly high potency as an antagonist of CB₁ and CB₂ receptor agonists *in vitro*. *British Journal of Pharmacology* 150: 613-23
- Twelves C, Sabel M, Checketts D, Miller S, Tayo B, et al. 2021. A phase 1b randomised, placebo-controlled trial of nabiximols cannabinoid oromucosal spray with temozolomide in patients with recurrent glioblastoma. *British Journal of Cancer* 124: 1379-87

Bibliography

- Umar S, Sellin J, & Morris A. 2000. Increased nuclear translocation of catalytically active PKC-zeta during mouse colonocyte hyperproliferation. *American journal of physiology. Gastrointestinal and liver physiology* 279 G223-37
- Verhaak RGW, Hoadley KA, Purdom E, Wang V, Qi Y, et al. 2010. Integrated Genomic Analysis Identifies Clinically Relevant Subtypes of Glioblastoma Characterized by Abnormalities in PDGFRA, IDH1, EGFR, and NF1. *Cancer Cell* 17: 98-110
- Vermersch P, Trojano M. 2016. Tetrahydrocannabinol:Cannabidiol Oromucosal Spray for Multiple Sclerosis-Related Resistant Spasticity in Daily Practice. *Eur Neurol* 76: 216-26
- Volmar MNM, Cheng J, Alenezi H, Richter S, Haug A, et al. 2021. Cannabidiol converts NF- κ B into a tumor suppressor in glioblastoma with defined antioxidative properties. *Neuro-Oncology* 23: 1898-910
- Wang B, Wei H, Prabhu L, Zhao W, Martin M, et al. 2015. Role of Novel Serine 316 Phosphorylation of the p65 Subunit of NF- κ B in Differential Gene Regulation. *Journal of Biological Chemistry* 290: 20336-47
- Wang Q, Hu B, Hu X, Kim H, Squatrito M, et al. 2017. Tumor Evolution of Glioma-Intrinsic Gene Expression Subtypes Associates with Immunological Changes in the Microenvironment. *Cancer Cell* 32: 42-56.e6
- Watts GS, Pieper RO, Costello JF, Peng YM, Dalton WS, Futscher BW. 1997. Methylation of discrete regions of the O6-methylguanine DNA methyltransferase (MGMT) CpG island is associated with heterochromatinization of the MGMT transcription start site and silencing of the gene. *Molecular and Cellular Biology* 17: 5612-19
- Weller M, Van Den Bent M, Tonn JC, Stupp R, Preusser M, et al. 2017. European Association for Neuro-Oncology (EANO) guideline on the diagnosis and treatment of adult astrocytic and oligodendroglial gliomas. *The Lancet Oncology* 18: e315-e29
- Wen PY, Weller M, Lee EQ, Alexander BM, Barnholtz-Sloan JS, et al. 2020. Glioblastoma in adults: a Society for Neuro-Oncology (SNO) and European Society of Neuro-Oncology (EANO) consensus review on current management and future directions. *Neuro-Oncology* 22: 1073-113
- Xiao G, Fong A, Sun S-C. 2004. Induction of p100 Processing by NF- κ B-inducing Kinase Involves Docking I κ B Kinase α (IKK α) to p100 and IKK α -mediated Phosphorylation. *Journal of Biological Chemistry* 279: 30099-105
- Xiao H, Goldthwait DA, Mapstone T. 1994. The identification of four protein kinase C isoforms in human glioblastoma cell lines: PKC alpha, gamma, epsilon, and zeta. *J Neurosurg* 81: 734-40
- Xiong W, Cui T, Cheng K, Yang F, Chen S-R, et al. 2012. Cannabinoids suppress inflammatory and neuropathic pain by targeting α 3 glycine receptors. *Journal of Experimental Medicine* 209: 1121-34
- Yamaoka S, Courtois G, Bessia C, Whiteside ST, Weil R, et al. 1998. Complementation Cloning of NEMO, a Component of the I κ B Kinase Complex Essential for NF- κ B Activation. *Cell* 93: 1231-40
- Yao H, Hwang J-W, Moscat J, Diaz-Meco MT, Leitges M, et al. 2010. Protein Kinase C ζ Mediates Cigarette Smoke/Aldehyde- and Lipopolysaccharide-induced Lung Inflammation and Histone Modifications. *Journal of Biological Chemistry* 285: 5405-16
- Young RM, Jamshidi A, Davis G, Sherman JH. 2015. Current trends in the surgical management and treatment of adult glioblastoma. *Ann Transl Med* 3: 121
- Yu H, Lin L, Zhang Z, Zhang H, Hu H. 2020. Targeting NF- κ B pathway for the therapy of diseases: mechanism and clinical study. *Signal Transduction and Targeted Therapy* 5

Bibliography

- Zeligs KP, Neuman MK, Annunziata CM. 2016. Molecular Pathways: The Balance between Cancer and the Immune System Challenges the Therapeutic Specificity of Targeting Nuclear Factor- κ B Signaling for Cancer Treatment. *Clinical Cancer Research* 22: 4302-08
- Zhang Y, Dube C, Gibert M, Cruickshanks N, Wang B, et al. 2018. The p53 Pathway in Glioblastoma. *Cancers* 10: 297
- Zhong H, May MJ, Jimi E, Ghosh S. 2002. The Phosphorylation Status of Nuclear NF- κ B Determines Its Association with CBP/p300 or HDAC-1. *Molecular Cell* 9: 625-36
- Zhong H, Suyang H, Erdjument-Bromage H, Tempst P, Ghosh S. 1997. The Transcriptional Activity of NF- κ B Is Regulated by the I κ B-Associated PKAc Subunit through a Cyclic AMP-Independent Mechanism. *Cell* 89: 413-24
- Zuardi AW. 2006. History of cannabis as a medicine: a review. *Revista Brasileira de Psiquiatria* 28: 153-57

Danksagung

Allen vorweg möchte ich meinem Doktorvater Prof. Dr. rer. nat. Rainer Glaß für die Aufnahme in seine Forschungsgruppe, das Inspirieren an der wissenschaftlichen Forschung, die stetige Unterstützung und die Leitung meiner Arbeit danken.

Ebenso möchte ich meinem Betreuer PD Dr. Roland Kälin dafür danken, dass er immer für Fragen offen war und unterstützend bei Problematiken Rat gegeben hat.

Der chemisch-technischen Assistentin Stefanie Lange möchte ich für die Einarbeitung in die Laborarbeit sowie die organisatorische Unterstützung im Labor danken.

Daneben möchte ich noch Dr. Huabin Zhang, Dr. Jiying Cheng, Dr. Min Li, Dr. Dongxu Zhao, Dr. Linzhi Cai, Dr. Sabrina Kirchleitner, Robin Wechter, Lena Schumacher und insbesondere Enio Barçi für den Austausch von Informationen und anregenden wissenschaftlichen Diskussionen danken, aber auch dafür, dass sie dazu beigetragen haben, dass die Zeit in der Forschungseinrichtung immer ein besonderer Abschnitt meines Lebens gewesen sein wird.

Zuletzt möchte ich noch meiner Familie und Freunden für die moralische Unterstützung danken, die mir auch in schwierigeren Zeiten immer wieder neuen Antrieb gegeben haben.

Eidesstattliche Versicherung

Richter, Sven

Name, Vorname

Ich erkläre hiermit an Eides statt, dass ich die vorliegende Dissertation mit dem Thema

CBD as a therapeutic agent for malignant glioma

selbständig verfasst, mich außer der angegebenen keiner weiteren Hilfsmittel bedient und alle Erkenntnisse, die aus dem Schrifttum ganz oder annähernd übernommen sind, als solche kenntlich gemacht und nach ihrer Herkunft unter Bezeichnung der Fundstelle einzeln nachgewiesen habe.

Ich erkläre des Weiteren, dass die hier vorgelegte Dissertation nicht in gleicher oder in ähnlicher Form bei einer anderen Stelle zur Erlangung eines akademischen Grades eingereicht wurde.

München, 25.02.2026

Ort, Datum

Sven Richter

Unterschrift Sven Richter

Richter, Sven

Name, Vorname

Hiermit erkläre ich, dass die elektronische Version der eingereichten Dissertation mit dem

Titel:

CBD as a therapeutic agent for malignant glioma

in Inhalt und Formatierung mit den gedruckten und gebundenen Exemplaren übereinstimmt.

München, 25.02.2026

Ort, Datum

Sven Richter

Unterschrift Sven Richter